molecular pharmaceutics

Article

A Lithocholic Acid-Based Peptide Delivery System for Enhanced Pharmacological and Pharmacokinetic Profile of Xenopus GLP-1 Analogs

Jing Han, Xinyu Chen, Li-Ming Zhao, Junjie Fu, Lidan Sun, Ying Zhang, Feng Zhou, and Yingying Fei

Mol. Pharmaceutics, **Just Accepted Manuscript** • DOI: 10.1021/acs.molpharmaceut.8b00336 • Publication Date (Web): 25 May 2018

Just Accepted

ACS Publications

is published by the American Chemical Society. 1155 Sixteenth Street N.W., Washington, DC 20036

Title:

A Lithocholic Acid-Based Peptide Delivery System for Enhanced Pharmacological and Pharmacokinetic Profile of *Xenopus* GLP-1 Analogs

Authors:

Jing Han,[a*] Xinyu Chen,[a] Liming Zhao,[a] Junjie Fu,[b*] Lidan Sun,[c*] Ying Zhang,[a] Feng Zhou,[a] Yingying Fei[a]

Affiliation and Address:

[a]School of Chemistry and Materials Science, Jiangsu Normal University, Xuzhou 221116, PR China

[b]Department of Medicinal Chemistry, School of Pharmacy, Nanjing Medical University, Nanjing 211166, PR China

[c]Department of Pharmaceutics, College of Medicine, Jiaxing University, Jiaxing 314001, PR China

***Corresponding Authors**

E-mail: **hj1986424@jsnu.edu.cn** (Jing Han)

E-mail: **jfu@njmu.edu.cn** (Junjie Fu)

E-mail: **sunlidan19890113@126.com** (Lidan Sun)

Table of Contents

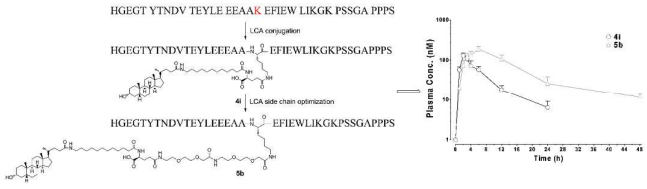

ABSTRACT

GLP-1 analogs suffer from the main disadvantage of a short *in vivo* half-life. Lithocholic acid (LCA), one of the four main bile acids in human body, possesses a high albumin binding rate. We therefore envisioned that a LCA-based peptide delivery system could extend the half-life of GLP-1 analogs by facilitating the noncovalent binding of peptides to human serum albumin. Based on our previously identified *Xenopus* GLP-1 analogs (**1**–**3**), a series of LCA modified *Xenopus* GLP-1 conjugates were designed (**4a**–**r**), and the bioactivity studies of these conjugates were performed to identify compounds with balanced *in vitro* receptor activation potency and plasma stability. **4c**, **4i** and **4r** were selected and their LCA side chain was optimized to further increase their stability, affording **5a**–**c**. Compound **5b** showed increased albumin affinity and prolonged *in vitro* stability than **4i** and liraglutide. In *db/db* mice, **5b** exhibited comparable hypoglycemic and insulinotropic activity to liraglutide and semaglutide. Importantly, the enhanced albumin affinity of **5b** resulted in a prolonged *in vivo* antidiabetic duration. Finally, chronic treatment investigations of **5b** demonstrated the therapeutic effects of **5b** on HbA1c, body weight, blood glucose and pancreatic endocrine deficiencies on *db/db* mice. Our studies revealed **5b** as a promising antidiabetic candidate. Furthermore, our study suggests the derivatization of *Xenopus* GLP-1 analogs with LCA represents an effective strategy to develop potent long-acting GLP-1 receptor agonists for the treatment of type 2 diabetes.

Keywords: Glucagon-like peptide-1; Type 2 diabetes; Lithocholic acid

Introduction

Type 2 diabetes mellitus (T2DM) is a chronic metabolic disease characterized by sustained hyperglycemia due to impaired insulin secretion, insulin resistance in peripheral tissues, and increased glucose output by the liver.[1-3] Chronic hyperglycemia can cause some health problems such as cardiovascular disease and nephropathy.[4-6] Unfortunately, most of the traditional drugs targeting T2DM suffer from several side effects such as hypoglycemia and/or weight gain.[7] New therapeutic agents that not only control progressive hyperglycemia but also have the potential to counter the weight gain and pancreatic endocrine function loss are in continuing demand. Glucagon-like peptide-1 (GLP-1), an incretin hormone secreted from intestinal L-cells, can stimulate insulin secretion without hypoglycemia risk, reduce food intake and appetite, and inhibit gastric emptying.[8, 9] However, the short *in vivo* half-life ($t_{1/2}$) of endogenous GLP-1 (~2 min) is not suitable for therapeutic application.[10, 11] Intensive research efforts have been made to develop GLP-1 derivatives with optimized pharmacokinetic profiles.[12] Currently six GLP-1 receptor agonists have been approved, including liraglutide, semaglutide, exenatide, etc., and many other agonists are in clinical trials.[13-15] However, most of them are based on the scaffold of native GLP-1 or exendin-4.

In search of novel incretin hormone as therapeutic agents for T2DM, we focused our research efforts on *Xenopus* GLP-1 as a peptide hormone backbone that is distinct from GLP-1 and exendin-4.[16] In our previous research, we successfully identified three *Xenopus* GLP-1 analogs (**1**–**3**, Figure 1) with prominent *in vitro* GLP-1 receptor activation potency and *in vivo* hypoglycemic activity. However, similar to other incretin hormones, the clinical utility of these analogs is limited

by their short half-lives. The introduction of a PEG moiety to **1**–**3** increased their half-lives, but only to a moderate extent due to the limited size of PEG (Mw = 1–5 ka).[17-19]

Albumin binding molecules such as fatty acids are able to improve the pharmacokinetic properties of peptides by facilitating the physical interactions between human serum albumin (HSA) and peptides.[20, 21] For example, lipidation strategy has been successfully used in clinical to afford liraglutide and semaglutide. Bile acid plays an important role in the absorption and solubilization of lipophilic vitamins and dietary fat, and could promote GLP-1 secretion through TGR5, a cell-surface bile acid receptor.[22, 23] In addition, previous reports revealed that bile acid possessed a high albumin binding rate.[24] There are four main bile acids in human, including cholic acid (CA), chenodeoxycholic acid (CDCA), deoxycholic acid (DCA) and lithocholic acid (LCA). It has been reported that the albumin binding affinity of bile acids decreases as the number of hydroxy groups increases, as reflected by the lower albumin binding percentage of CA (three hydroxyls) versus LCA (one hydroxyl).[25] These characteristics make LCA an ideal small molecule albumin binder for peptide modification. We envision that the covalent coupling of LCA to *Xenopus* GLP-1 analogs might offer a practical and alternative means to develop novel long-acting GLP-1 receptor agonists.

It is known that the spacer between the small molecule and the polypeptide plays an important role in albumin binding.[13] In the present study, based on our previous research experience on mycophenolic acid (MPA),[26] three different spacers were used to connect LCA and peptides **1**–**3** at residues Lys_{20} and Lys_{28}, affording eighteen (3 × 3 × 2) LCA-*Xenopu*s GLP-1 conjugates (**4a**–**r**, Figure 1). Compounds **4c**, **4i** and **4r** with high *in vitro* plasma stability, potent receptor activation potency, and prominent hypoglycemic activity were further modified with 8-amino-3,6-dioxa-octanoic acid (abbreviated as O2Oc) spacers to gain additional benefits in

hypoglycemic duration, giving **5a**–**c** (Figure 5). The anti-diabetic potency, insulinotropic activity, *in vivo* stability, acute toxicity, and chronic treatment effects of these conjugates were extensively explored.

Materials and methods

Animals

C57BL/6J-m$^{+/+}$ Lepr^{db} (*db/db*) mice (male, 30−40 g, 7−9 weeks) were obtained from Model Animal Research Center of Nanjing University (Jiangsu, China). Kunming mice (male, 20−30 g, 6−8 weeks) and Sprague-Dawley (SD) rats (male, 9–11 weeks, 200–250 g) were obtained from Comparative Medical Center of Yangzhou University (Jiangsu, China). Normal Kunming mice are non-diabetic and wildly used in preliminary *in vivo* antidiabetic activity research. SD rats are the species commonly used in pharmacokinetic research. *db/db* mice is a rodent model of type 2 diabetes wildly used in diabetes research. Six mice or three rats were housed in a single polycarbonate solid-bottomed cage and all animals were housed in specific pathogen free (SPF) facilities under controlled conditions (25 ± 3°C, reverse 12 h-light-dark cycle). All animals were acclimatized for 7 days before used in the studies. The water and food (standard laboratory chow) were provided *ad libitum* throughout the study except otherwise noted. The experimental procedures conducted on animals were performed as humane as possible and in accordance with the Laboratory Animal Management Regulations in China, the Guide for the Care and Use of Laboratory Animals published by the National Institutes of Health (revised 2011), and approved by Jiangsu Normal University ethical committee.

Materials

Fmoc protected amino acids, Rink amide MBHA resin, N,N'-diisopropylcarbodiimide (DIC), N-Hydroxybenzotriazole (HOBt), GLP-1, liraglutide and semaglutide were obtained from GL Biochem Ltd. (Shanghai, China). Fmoc-β-Ala-OH, Fmoc-6-Ahx-OH and Fmoc-12-Ado-OH were purchased from Sigma-Aldrich (Saint Louis, MO, USA). Fmoc-8-amino-3,6-dioxa-octanoic acid (Fmoc-AEEAc-OH) was purchased from Bachem (Bachem AG, Switzerland). cAMP dynamic kit was obtained from Cisbio (Bedford, MA, USA), and mouse insulin ELISA kit was obtained from Nanjing Jiancheng Bioengineering Institute (Jiangsu, China). Other reagents, unless specific indicated, were purchased from Sigma-Aldrich and used directly.

Peptide synthesis

All *Xenopus* GLP-1 analogues were synthesized by standard SPPS using the Fmoc strategy on a PSI-200 semi-automated peptide synthesizer (Peptide Scientific Inc., USA).[27] Resins used were Rink amide MBHA resin with a loading of 0.38 mmol·g^{-1}. For conjugates **4a**–**r**, the Lys to be modified was replaced with Fmoc-Lys(Dde)-OH and the N-terminal was replaced with Boc-His(Trt)-OH. The Dde protection group was selectively removed by washing 5 times for 15 min with 2% hydrazine hydrate/DMF (v/v, 7 mL). Next, Fmoc-Glu-OtBu (0.4 eq.), Fmoc-β-Ala-OH, Fmoc-6-Ahx-OH or Fmoc-12-Ado-OH (0.4 eq.), and LCA (0.4 eq.) were added to the reaction vessel in sequential and the coupling reaction was performed by using DIC/HOBT (0.4 eq.) for 2–3 h at 25°C. For conjugates **5a**–**c**, the synthetic route was similar, except that after Dde deprotection, Fmoc-AEEAc-OH was firstly added and coupled using the same condition. Then Fmoc-Glu-OtBu, Fmoc-12-Ado-OH and LCA were added and coupled in order. Finally, the crude

peptides were cleaved from the resin by using Reagent K (EDT/phenol/water/thioanisole/TFA, 2.5:5:5:5:82.5, 5 mL). Crude products were precipitated using ether, purified by semi preparative RP-HPLC (Shimadzu LC-20AP), and characteristic by HPLC (Agilent 1260 infinity) and MS (Bruker MicroTOF Q2).

Functional assay

Agonism of peptides for the GLP-1 receptor was measured by functional assays using a stable HEK-293 cell line expressing human GLP-1 receptor.[18] Intracellular cAMP content was determined by using Cisbio cAMP dynamic kit based on HTRF (homogeneous time-resolved fluorescence technology) using a multilabel reader (Envision 2,104, PerkinElmer). For preparation, cells were grown in DMEM medium supplemented with 0.5% FBS, 20 mM HEPES, 50 units·mL^{-1} penicillin, 2 mM glutamine and 50 μg·mL^{-1} streptomycin. Before testing, cells were plated in 96-well plates, and tested compounds were diluted in assay buffer and added to the cells to reach final concentrations of 1×10^{-13}–1×10^{-7} M. After addition of HTRF reagents and incubation at 37°C for 60 min, the fluorescence data in cells were measured and converted into cAMP concentration by using a standard curve. The potency of tested peptides was quantified by EC_{50} using GraphPad Prism version 5.0 (San Diego, CA).

IPGTT in Kunming mice

The IPGTT test on Kunming mice was used a previous described method.[28] In brief, male mice were randomly divided (n = 6) and acclimate for 7 days. One day before the experiment, mice were fasted for 12 h, followed by *i.p.* injected of saline, GLP-1, liraglutide, **1**–**3**, **4a**–**r** and **5a**–**c** (25

nmol·kg^{-1}, -10 or -30 min). Glucose was *i.p.* loaded at 0 min, and blood glucose levels were determined using a Sannuo glucometer (GA-3, China) by collecting blood from the tail at -30 or -10, 0, 15, 30, 45, 60, and 120 min.

Metabolism studies in rat plasma

The *in vitro* stability studies of liraglutide, **4a**−**r** and **5a**−**c** were conducted in rat plasma as previously described with slight modifications.[29] The initial concentration of the tested peptides was 1000 ng·mL^{-1} and incubation was performed for 72 h at 37°C with gentle shaking. After 4, 8, 12, 24, 48 and 72 h, a sample (100 μL) was collected and mixed with 200 μL acetonitrile containing 0.5% formic acid for plasma protein precipitation. LC−MS/MS analysis (Applied Biosystems Sciex API-4000) was conducted using linear gradients and peptides were detected by multiple reaction monitoring (MRM). The degradation curves were plotted by three independent experiments (n = 3).

Albumin binding test

The relative albumin binding abilities of **4i**, **5b**, liraglutide and semaglutide were determined by high-performance affinity chromatography (HPAC) using CHIRALPAK HSA column (Chiral Technologies Europe) using a previous described method with some modifications.[30] Briefly, chromatographic separation was conducted on Agilent 1260 HPLC using an immobilized HSA column (2 × 50 mm, 5 μm). Tested samples were injected into the column under 25°C and the isocratic mobile phase was 20% 2-propanol in potassium phosphate buffer (20 mM, pH 7.0). Detection of the peptides was carried out at 214 nm UV. The retention times (t_R) of tested peptides

were repeated in three independent experiments and the retention factor (*k*') was calculated by using $(t_R-t_M)/t_M$, where t_M is the column void time and t_R is the retention time of the tested peptides.

Pharmacokinetic studies

Pharmacokinetics studies of **4i** and **5b** were used previous described method with some modification.[9] Male SD rats (n = 3) of approximately 200–250 g were allowed to acclimatize for 7 days. After fasting 12 h, **4i** and **5b** (50 nmol·kg^{-1}) were *s.c.* injected using 1:1 20 M sodium phosphate buffer/propylene glycol (pH = 7.4) dosing vehicle. Serial blood samples (100–200 μL) were collected from fundus venous plexus in microcentrifuge tubes (EDTA containing) at 0, 1, 2, 3, 4, 6, 12, 24 and 48 h. Plasma was obtained by centrifugation and stored at −20°C until analysis. The plasma proteins were precipitated by adding two volumes of acetonitrile (containing 0.5% formic acid) followed by centrifuged (14000 rpm, 10 min), and 10 μL of supernatants were analyzed by LC−MS/MS.

Glucose-lowering and insulinotropic tests in db/db mice

The glucoregulatory and insulinotropic abilities of liraglutide, semaglutide and **5b** were determined on *db/db* mice by IPGTT, using a previous described method.[31] For the study, male *db/db* mice (30−40 g, 7−8 weeks) were randomly divided (n = 6) and acclimatized for 7 days. After fasting 18 h, mice were weighed and saline, liraglutide, semaglutide and **5b** (25 nmol·kg^{-1}) were *i.p.* loaded 30 min prior to glucose load. At time 0 min mice were *i.p.* injected 1 g·kg^{-1} of glucose to initiate the IPGTT. The mice were bled from the tail vein at -30, 0, 15, 30, 45, 60, 90, 120 and 180 min. Blood glucose were immediately measured using Sannuo one-touch glucometer (GA-3, China).

For plasma insulin, the blood collected at 10, 15 and 20 min were centrifuged and mouse insulin ELISA kit (Nanjing Jiancheng Bioengineering Institute, Jiangsu, China) were used to assay the plasma insulin levels.

Pharmacodynamic studies

Male *db/db* mice ages 7−9 weeks with blood glucose levels over 15 mmol·L^{-1} were acclimatize for 7 days and mice were divided to 8 groups (n = 6) according to their non-fasting blood glucose levels.[32] On the experiment days, saline (control), liraglutide, semaglutide, and **5b** (25 or 150 nmol·kg^{-1}) were *i.p.* injected at 0 h. Mice were allowed to free access to standard rodent chow and water until experiment finished. The blood was drawn from the tail vein and non-fasting blood glucose concentrations were measured using Sannuo glucometer at 0, 0.5, 1, 2, 3, 4, 5, 6, 8, 10, 12, 24, 48 and 60 h. During the experiment, the food intake was also recorded during 0−24 h (at a dose of 25 nmol·kg^{-1}). The rodent chow was pre-weighed and the cumulated food intake in each group was recorded at 0, 0.5, 1, 2, 3, 4, 5, 6, 8, 10, 12 and 24 h.

Toxicity Assay

The *in vitro* toxicity of **5b** was determined by cell viability assay on rat pancreatic INS-1 cells, using a previous described method.[27] Briefly, cells were cultured in RPMI 1640 medium with 11.2 mM glucose and other supplements in a 5% CO_2 atmosphere at 37°C. For the measurement, cells were transferred to 96-well culture plates (~5000 cells/well). After incubate for 24 h, the cells were treated with saline, liraglutide, semaglutide (10 nM), or **5b** (10, 100, 1000 nM) followed by 24 h incubation. Then 3-(4,5-Dimethylthiazol-2-yl)-2,5-diphenyltetrazolium bromide (MTT, 5 mg·mL^{-1})

were added in the cells and incubate for 5 h at 37°C. Then media was removed to stop the reaction and DMSO was added to dissolve the purple formazan precipitate followed by 30 min gentle shaking. The cell viability was measured at 570 nm (optimum absorption of formazan) by Thermo spectrophotometer (Labsystems, MA, USA).

The acute *in vivo* toxicity test of **5b** was performed on male *db/db* mice (7−9 weeks, n = 3), as previously described.[27] Mice were randomly divided and acclimatized for 7 days. Before the experiment, mice were fasted for 18 h, and then *i.p.* loaded low dose of **5b** (100 $mg \cdot kg^{-1}$), high dose of **5b** (500 $mg \cdot kg^{-1}$) or equal volumes of saline (control). Food was provided immediately and mice were allowed to free access to water and food. On the second day, saline and different doses of **5b** were loaded again at the same time under the same administration route. After 24 h, mice were sacrificed and the blood was collected. The serum AST and ALT levels were measured using CHEMIX-180 Automatic Analyzer (Sysmex, Japan) based on kinetic rate method with Ningbo Medical System Biotechnology commercial kits (Ningbo, China).

Chronic treatment tests

Male *db/db* mice at an age of 8−9 weeks were housed in groups and 6 mice per cage. Mice were acclimatized for one week. Blood samples were collected and HbA1c levels were measured using chemistry analyzer based on the immunoagglutination inhibition method (DCA 2000+, Bayer Diagnostics, USA) and then mice were divided matched HbA1c.[33] Saline and liraglutide (25 $nmol \cdot kg^{-1}$) were twice daily *s.c.* injected at 8 AM and 8 PM, and **5b** (25 $nmol \cdot kg^{-1}$) was once daily *s.c.* injected at 8 AM for 35 days. HbA1c and plasma insulin concentrations were measured weekly using DCA 2000+ chemistry analyzer and mouse insulin ELISA kit, respectively. Blood glucose

levels were determined using Sannuo glucometer at 12 PM every two days. Food intake and body weight change were recorded every day at 6 PM. At day 36, mice were fasted 18 h and subjected to an IPGTT. Glucose (1 $g \cdot kg^{-1}$) was *i.p.* loaded and blood glucose levels in each group were monitored at 0, 15, 30, 60, 90, 120 and 180 min. A terminal blood sample was used for determination of AST and ALT using the same method described above. Mice were allowed to recover 1 day after IPGTT and then sacrificed. The pancreas was removed and fixed in paraformaldehyde (4%) 12 h at 4°C. The detail methodology of insulin immunohistochemistry has been described elsewhere.[34] The integrated optical density (IOD) values of insulin were determined by Image-pro plus 6.0 (Media Cybernetics, Inc., Rockville, MD, USA).

Data Analysis

Data are presented as Means ± SD. The pharmacokinetic profiles of **4i** and **5b** were determined using the Bioavailability Program Package software 2.2 (Center of Drug Metabolism and Pharmacokinetics, China Pharmaceutical University) and other pharmacology data analyses were performed using GraphPad Prism 5. Statistical significance analyses were performed by one-way ANOVA for comparisons between multiple groups followed by the Tukey's post hoc tests if F achieved statistical significance ($P < 0.05$) and there was no significant variance in homogeneity. $P < 0.05$ was considered statistically significant.

Results

*Design and synthesis of LCA-Xenopus GLP-1 conjugates **4a**–**r***

To test the hypothesis of using LCA as an albumin binding molecule to improve the pharmacokinetics of GLP-1 analogs, conjugates of LCA and peptides **1**–**3** were designed. *Xenopus* GLP-1 analogs **1**–**3** were identified in our previous work. The C-terminal regions of exendin-4 (PSSGA PPPS) and lixisenatide (PSSGA PPSKK KKKK) were introduced to peptide **1** to afford peptides **2** and **3**, respectively, aiming to further improve the bioactivity of **1**.[35,36] Based on our previous research experience, the lipophilicity of the linker could have an important impact on albumin binding affinity. Hence, three ω-amino acids with different chain lengths (C2, C5 and C11) were employed as the linkers. To compensate the overall decrease in water solubility caused by LCA conjugation, γ-glutamic acid (γGlu) was attached to the linker and the γ-carboxyl group was connected directly to the Lys residues of peptides through an amide bond. Lys_{20} and Lys_{28} of peptides **1**–**3** were chosen for site specific conjugation based on our pervious structure-activity relationships (SAR) studies on *Xenopu*s GLP-1 analogs. A total of eighteen LCA-*Xenopu*s GLP-1 conjugates (**4a**–**r**, Figure 1) were prepared using the synthetic route shown in Scheme 1. Briefly, C-terminus peptide amides were obtained by Fmoc solid-phase peptide synthesis (SPPS) on Rink Amide MBHA resins. Site-specific LCA conjugation at the side chain of Lys_{20} and Lys_{28} was achieved by incorporating Fmoc-Lys(Dde)-OH into these position, and the Dde protecting group was selectively removed by using 2% hydrazine hydrate/DMF (v/v). Fmoc-Glu-OtBu was attached to the side chain amino group of Lys, followed by deprotection of Fmoc and connection of N-Fmoc protected ω-amino acids (β-alanine, 6-aminocaproic acid, and 12-aminolauric acid). After removal of Fmoc, the ω-amino groups were linked to the carboxyl group of LCA to furnish the conjugation. The crude products were cleaved from the solid support and purified by semi preparative RP-HPLC

(Shimadzu, LC-20AP). The purified products were characterized by HPLC (Agilent 1260) and Bruker MicroTOF MS (see Supporting Information).

Put Figure 1 here

Put Scheme 1 here

In vitro and in vivo biological activities of **4a**–**r**

As cyclic AMP (cAMP) is the main effector of GLP-1 induced insulin secretion in beta cells, it was selected as a probe to test the GLP-1 receptor activating potencies of our peptides (**4a**–**r**) by using recombinant HEK-293 cells stably expressing human GLP-1 receptors.[3] For dose-response tests, HEK-293 cells were treated with tested compounds at various concentrations. After 60 min incubation at 37°C, the produced cAMP was determined by cAMP dynamic 2 kit. The concentration response curves of GLP-1 and representative LCA-*Xenopus* GLP-1 conjugates are shown in Figure 2. The EC_{50} values of all the tested peptides are summarized in Table 1. Most of the LCA-*Xenopus* GLP-1 conjugates showed a high receptor activation potency. Interestingly, compounds **4a**, **4d**, **4g**, **4j**, **4m** and **4p**, all of which possess a *β*-alanine moiety as the linker, exhibited comparable potency to their parent peptides, indicating that a shorter alkyl chain was more favorable for receptor activation potency. Increasing the alkyl length of linker had a negative impact on potency, and the results are in accordance with our previously reported date on dicoumarol GLP-1 conjugates.[37] Furthermore, for conjugates **4a**–**l**, which were derived from **1** and **2**, LCA conjugation at Lys_{20} was more beneficial for receptor activation. However, in case of **4m**–**r**, which were derived from **3**, the conjugate site had no significant effects.

Put Figure 2 here

Put Table 1 here

It is known that high expression of GLP-1 receptor in HEK-293 cells could promote the binding and avidity of tested compounds *in vitro*, but the situation *in vivo* may be different. To further validate the results of the *in vitro* receptor activation potency experiments, the *in vivo* glucose-lowering activities of **4a**–**r** were studied using the intraperitoneal glucose tolerance testing (IPGTT) in Kunming mice. As illustrated in Figure 3, following an intraperitoneal glucose challenge, the blood glucose concentrations were significantly reduced in all treatment groups compared with the saline control. Blood glucose levels in the saline treated group rapidly increased over 20 $mmol \cdot L^{-1}$ at 15 min after glucose administering (2 $g \cdot kg^{-1}$), while mice treated with GLP-1 or **4a**–**r** showed rapid glucose clearance kinetics, and the average blood glucose levels were reduced to < 10 $mmol \cdot L^{-1}$ at 45 min after the glucose challenge. Particularly, the *in vivo* antidiabetic effects of **4c** and **4i**, which have the longest alkyl chain linker, were similar to GLP-1, and the glucose-lowering activity of **4r** was significantly better than GLP-1 ($P < 0.001$, Table 1). Interestingly, although the *in vitro* EC_{50} values of **4b**, **4h**, **4o** and **4r** are higher than GLP-1, their *in vivo* $AUC_{glucose}$ values are lower than that of GLP-1 (Table 1), suggesting improved stabilities of the LCA-*Xenopus* GLP-1 conjugates *in vivo*.

Put Figure 3 here

In vitro stability

The *in vitro* plasma stability assays were performed prior to resource-demanding pharmacokinetic experiments for a preliminary evaluation of the stabilities of **4a**–**r**, using liraglutide as the positive control. Liraglutide and **4a**–**r** were incubated with rat plasma at 37°C over 72 h, and aliquots collected during the incubation process were analyzed by LC-MS/MS. As shown in Figure 4 and Table 2, the introduction of LCA was found to be effective in stability enhancement of *Xenopus* GLP-1 analogs. A straightforward relationship was observed between the alkyl chain length of the linker and the *in vitro* half-lives for compounds **4a**–**r**, whereas the LCA conjugation position had no significant effects. It should be noticed that the plasma stabilities of **4m**–**r** (derived from **3**) were lower than **4g**–**l** (derived from **2**). This is opposite to the results reported for exendin-4 and lixisenatide, in which the C-terminal six Lys extension has a positive effect on stability.[38, 39] Taken together, considering the high plasma stability of **4c**, **4i** and **4r**, which is essential for the long-acting *in vivo* hypoglycemic activity, together with the potent receptor activation potency and *in vivo* glucose-lowering activity of **4c**, **4i** and **4r**, these three conjugates were selected as lead compounds for further optimization.

Put Figure 4 here

Put Table 2 here

Optimization of LCA side chain for further in vivo stability improvement

The above results demonstrated that LCA conjugation extended the *in vitro* half-lives of **4c**, **4i** and **4r** to ~40 h. However, this duration is still far shorter than the *in vivo* half-life of HSA, which is

known to be up to three weeks.[40] Therefore, we envisioned that the *in vivo* half-life of LCA-*Xenopus* GLP-1 conjugates could be further improved by a second step modification. In previous reports, through the replacement of the C16 fatty acid by C18 di-acid, the substitution of Ala_2-Glu_3 with Aib_2-Glu_3, and the introduction of two O2Oc spacers between Lys_{28} and γGlu-C18 di-acid, the half-life of liraglutide was significantly improved, and the afforded semaglutide has been approved recently by FDA to be used as once-weekly anti-diabetic therapeutic. Furthermore, unlike other hydrophobic small molecules (e.g. fatty acid, dicoumarol) which could increase the overall lipophilicity of the peptides and raise solubility issues, the high hydrophilic property of O2Oc could decrease the hydrophobicity of peptides, bringing additional benefits. Inspired by these results, we explored the possibility of introducing the O2Oc spacer to the LCA side chain of the selected compounds (**4c**, **4i** and **4r**) to further improve their stability.

As shown in Figure 5, two O2Oc spacers were introduced into the side chain of **4c**, **4i** and **4r**, and the O2Oc spacers were placed between the Lys_{20} or Lys_{28} and γGlu-C11-LCA of **4c**, **4i** and **4r**, affording **5a**–**c**. The synthetic procedure (Scheme 2) was similar to that of **4a**–**r**, except that after the selective removal of Dde, Fmoc protected 8-amino-3,6-dioxa-octanoic acid (Fmoc-AEEAc-OH) was firstly connected to peptide backbones using standard solid-phase conditions. The affording crude products were cleaved, purified and characterized using the same method described above (see Supporting Information).

Put Figure 5 here

Put Scheme 2 here

*Stability and biological activity tests of **5a–c***

The *in vitro* stabilities of **5a–c** were tested using the same experimental procedures as described above. As shown in Figure 6A, the *in vitro* stabilities of **5a–c** were significantly improved as compared with **4c**, **4i** and **4r**. In particular, **5b** was found to be extremely stable, and about 53% of intact peptide was still found after a 72 h incubation. Next, to assess the impact of O2Oc spacer on the biological activities of **5a–c**, the *in vitro* receptor activation potency and *in vivo* glucose-lowering activities of **5a–c** were investigated. As shown in Figure 6B, the introduction of O2Oc spacers was well-tolerated with respect to GLP-1 receptor activation potency, as reflected by the high potency of **5a** (EC_{50} = 1.55 ± 0.32 nM), **5b** (EC_{50} = 0.70 ± 0.12 nM) and **5c** (EC_{50} = 0.49 ± 0.09 nM). Importantly, the potency of **5b** and **5c** were comparable to that of liraglutide (EC_{50} = 0.64 ± 0.15 nM). The IPGTT in Kunming mice showed that the hypoglycemic activity of **5a** was less potent than liraglutide, whereas **5b** and **5c** treatments effectively reduced blood glucose and showed better antihyperglycemic activities than liraglutide (Figures 6C and D). These results indicate that the biological activities of **5a–c** retain after the introduction of O2Oc spacers. Considering its high stability and potency, **5b** was finally selected for the following studies.

Put Figure 6 here

Albumin binding and pharmacokinetic studies

To evaluate whether the albumin binding ability of **5b** was enhanced after O2Oc modification, the *in vitro* albumin affinity of **5b** was tested and compared with its non-O2Oc counterpart **4i**, using liraglutide and semaglutide as the positive controls. Instead of measuring the absolute binding rates

between the peptides and serum albumin, we evaluated the albumin binding affinities of liraglutide, semaglutide, **4i** and **5b** by high performance affinity chromatography (HPAC) analysis on the CHIRALPAK HSA column, using the retention factor (*k*') as the indicator for albumin affinity. The value of *k*' was calculated as $(t_R-t_M)/t_M$, where t_M is the column void time and t_R is the retention time of the tested peptides. As illustrated in Figure 7A, the *k*' values of liraglutide and **4i** were ~12.5 and ~11.4, respectively. The albumin affinity of **5b** (*k*' = ~18.7) was higher than **4i** and liraglutide, but still lower than semaglutide (*k*' = ~21.9). Next, we investigated whether the high albumin affinity observed for **5b** resulted in better pharmacokinetic (PK) effects *in vivo*. The PK properties of **4i** and **5b** were evaluated in SD rats (n = 3 per group) by *s.c.* injection of the peptides (50 $nmol \cdot kg^{-1}$). As illustrated in Figure 7B, **5b** exhibited a half-life ($t_{1/2}$ = 11.0 ± 1.2 h) ~2.0 fold longer than that of **4i** ($t_{1/2}$ = 5.4 ± 1.0 h), and the observed time of **5b** to reach maximum plasma concentration (T_{max}) was ~6.0 h, which was longer than that of **4i** (~2.3 h). Moreover, the maximum plasma concentration (C_{max}) of **5b** (188.1 ± 30.7 nM) was higher than that of **4i** (130.7 ± 18.9 nM). In summary, the introduction of O2Oc spacer to **4i** dramatically increased the albumin affinity and led to protracted *in vivo* half-life and improved PK behaviors.

Put Figure 7 here

Hypoglycemic and insulinotropic activity tests in db/db mice

We next examined the anti-diabetic and insulinotropic effects of **5b** by IPGTT in *db/db* mice, a type 2 diabetic model, using liraglutide and semaglutide as the positive controls. As shown in Figure 8A, the average blood glucose levels in the saline group rapidly increased over 20 $mmol \cdot L^{-1}$

and maintained a hyperglycemic state (> 20 mmol·L^{-1}) during 15–90 min post *i.p.* glucose challenge. However, liraglutide, semaglutide and **5b** treatments significantly potentiated glucose stimulated insulin release, resulting in decreased glucose. The average blood glucose levels in semaglutide and **5b** groups were slightly lower than that in liraglutide group at 15, 30, 45 and 60 min post glucose challenge. Furthermore, $AUC_{glucose}$ values revealed that the hypoglycemic effects of semaglutide and **5b** were comparable and were slightly better than liraglutide, but no significant differences were observed among liraglutide, semaglutide and **5b** treatmented groups (Figure 8B). Moreover, the plasma insulin levels in each group of mice were recorded at 10, 15 and 20 min post glucose challenge. As shown in Figures 8C, liraglutide, semaglutide and **5b** treated mice showed significantly increased insulin levels versus the saline group at 10, 15 and 20 min. In addition, the insulinotropic activities of liraglutide, semaglutide and **5b** were similar in *db/db* mice. These results indicated that the hypoglycemic and insulinotropic activities of **5b** were comparable to that of liraglutide and semaglutide.

Put Figure 8 here

Hypoglycemic duration and food intake tests in db/db mice

The anti-diabetic duration of **5b** was tested in non-fasted *db/db* mice and compared with that of liraglutide and semaglutide. As shown in Figure 9A, at the dose of 25 nmol·kg^{-1} (*i.p.*), the blood glucose levels in mice treated with liraglutide decreased rapidly. The normoglycemia state lasted for ~12 h, and then returned to hyperglycemia state at 24 h after injection. The normoglycemia state in groups treated with equimolar of semaglutide or **5b** lasted for > 24 h. Consistent with the albumin

binding results, both semaglutide and **5b** exhibited longer hypoglycemic durations than liraglutide. The glucose-lowering activities of semaglutide and **5b** were similar during 0–24 h. The hypoglycemic activity of **5b** decreased 48 h post injection, and became indistinguishable with saline group 60 h post injection, while the blood glucose levels in semaglutide group were still maintained below 15 mmol L^{-1} 60 h post injection. The $AUC_{glucose}$ values proved that the anti-diabetic duration effects of semaglutide and **5b** were significantly better than liraglutide ($P < 0.001$ and $P < 0.01$ *vs.* liraglutide, respectively, Figure 9B). Next, a further dose-response study clearly revealed that **5b** had a dose-dependent anti-diabetic efficacy. At the dose of 150 nmol·kg^{-1}, the antidiabetic duration of **5b** was up to 48 h, as reflected by the low blood glucose levels in **5b** groups at 48 h. However, the anti-diabetic duration of **5b** was still shorter than semaglutide at this dose. The $AUC_{glucose}$ data further proved that the hypoglycemic duration of **5b** was significantly longer than liraglutide ($P < 0.01$ *vs.* liraglutide) but still shorter than semaglutide (Figure 9D).

It is well known that both liraglutide and semaglutide had anorectic effects.[41] Thus, to evaluate the anorectic effect of **5b**, the food intakes in each group of mice were also recorded during the hypoglycemic duration tests (at the dose of 25 nmol·kg^{-1}, *i.p.*, recorded during 0–24 h). As shown in Figure 10A, compared with the saline group, liraglutide, semaglutide and **5b** treatments significantly reduced the food intake during 0–12 h. Obvious difference of food intake amount in each group of mice was observed 24 h post injection. Compared with the saline group, administration of liraglutide decreased the cumulative food intake by ~36%, while semaglutide and **5b** reduced food intake by ~56% and ~46%, respectively. The poorer PK profile of **5b** than semaglutide may be the main reason accounting for the less anorectic effect of **5b** at 24 h than semaglutide. Noticeably, **5b** had a better anorectic effect than semaglutide during 0–12 h, indicating

the potential of **5b** to be further developed into a long-acting anorectic agent after additional optimization.

Put Figure 9 here

Put Figure 10 here

Toxicity tests

The introduction of small molecules to GLP-1 analogs could effectively alter the PK profiles and improve the biological efficacy. However, another problem should be kept in mind is the potential toxicity brought by the small molecules. Particularly, previous researches have reported that the administration of LCA may lead to hepatoxicity.[42] Thus, both *in vitro* and acute *in vivo* toxicity tests were conducted to evaluate the toxicity of **5b**. The *in vitro* toxicity of **5b** was evaluated on INS-1 cells by MTT assay. The cells were exposed to 11.2 mM glucose (normal glucose condition) with 10 nM liraglutide or semaglutide or **5b** (10–1000 nM). As shown in Figure 10B, treatment with 10 nM liraglutide and semaglutide for 24 h did not reduce cell viability. The same trend was also observed for the cells treated with 10 or 100 nM of **5b**. Treatment with the highest concentration of **5b** (1000 nM) only slightly reduced the cell viability. Taken together, these results indicated the low toxicity of **5b** *in vitro*.

The *in vivo* toxicity of **5b** was further tested. Due to the limited **5b** supply, mice were used and only an acute toxicity test was conducted. Serum aspartate aminotransferase (AST) and alanine aminotransferase (ALT) were used as two important indicators for hepatic toxicity. As shown in Figures 10C and D, compared with the saline group, administration of 100 or 500 mg kg^{-1} of **5b** for

two days did not result in significant elevation of either AST or ALT level. Therefore, both the *in vitro* and *in vivo* toxicity tests suggested that the safety of **5b**.

Chronic studies in db/db mice

To further evaluate the potential therapeutic utility of **5b**, the chronic treatment effects of **5b** in *db/db* mice were tested. Considering the shorter anti-diabetic duration of **5b** as compared with semaglutide and the well characterized long-term treatment effects of liraglutide, we selected liraglutide as the positive control. Based on the hypoglycemic duration test of liraglutide and **5b**, liraglutide and **5b** (25 $nmol \cdot kg^{-1}$) were twice daily and once daily injected, respectively. Subcutaneous (*s.c.*) injection was used to better mimic the environment of clinical use. The *db/db* mice were divided with their well-matched HbA1c values which were tested by using a DCA 2000+ chemistry analyzer. As shown in Figure 11A, the HbA1c values in saline group gradually increased during the five-week treatment. In contrast, compared with day 0, treatment with liraglutide or **5b** prohibited the worsening of the HbA1c during the treatment period and lowered the HbA1c by ~1.7% and ~4.5% on day 35, respectively. The food intake and body weight change in each group of mice were recorded every day. As shown in Figures 11B and C, both liraglutide and **5b** potently reduced food intake and the anorectic effect of **5b** was slightly better than liraglutide from day 16. Consequently, the body weight change in liraglutide and **5b** groups were lower than that in the saline group, and the relative body weight reductions in liraglutide and **5b** treated mice were ~72% and ~84%, as compared with the saline group on day 36. Furthermore, both liraglutide and **5b** exhibited prominent effects on lowering non-fasting blood glucose concentrations, and these effects were accompanied by significantly enhanced non-fasting plasma insulin concentrations (Figures

11D and E). Liraglutide and **5b** did not differ in their effects on glucose-lowering and insulinotropic during the five-week treatment.

At the end of the study, we performed an IPGTT to evaluate the beneficial effects of liraglutide and **5b** treatments on glucose tolerance. As shown in Figure 11F, administration of liraglutide or **5b** resulted in improved glucose tolerance patterns, as reflected by the significantly decreased blood glucose levels compared with the saline group. The immunohistochemistry analysis of pancreata (Figure 12) revealed that the insulin in islets of saline treated mice was extremely reduced. However, in islets of the liraglutide or **5b** treated mice, the staining of insulin was significantly improved. The results of the immunohistochemistry indicated the beneficial treatment effects of liraglutide and **5b** on amelioration of pancreatic endocrine deficiencies. Importantly, we did not observe the hepatotoxicity of **5b** after the five-week treatment. The AST and ALT values in **5b** treated mice were similar to that in the saline and liraglutide groups, indicating again the safety of **5b** during chronic usage (Table 3).

Put Figure 11 here

Put Figure 12 here

Put Table 3 here

Discussion

Our previous research on *Xenopus* GLP-1 analogs (**1**–**3**), which could potently activate GLP-1 receptor and lower blood glucose, suggested the potential of these peptides to be developed as novel GLP-1 receptor agonists. However, the relatively poor pharmacokinetic profiles of these peptides

should be improved. In this study, we demonstrated a novel method to improve the stability of GLP-1 analogues through the introduction of the albumin binding molecule LCA. Eighteen novel LCA-*Xenopus* GLP-1 conjugates (**4a**–**r**) were designed and successfully synthesized using SPPS. Functional screening results showed that the LCA moiety was well tolerated by peptides **1**–**3**. SAR studies revealed that the potencies of **4a**–**r** decreased as the length of the alkyl chain linker increased. For conjugates (**4a**–**l**) derived from **1** and **2**, the conjugation position of the peptide also impacted the receptor activation potency, and Lys_{20} was preferred. However, for **4m**–**r** which were derived from **3**, the conjugation position had no significant impact on potency. This is an interesting finding, and the inconsistent SAR between **4a**–**l** and **4m**–**r** may result from the different C-terminal sequences between **1**–**2** and **3**. *In vivo* IPGTT tests revealed a similar SAR. Interestingly, some conjugates exhibited higher EC_{50} values than GLP-1 but showed lower $AUC_{glucose}$ values than GLP-1. To examine the *in vitro* stability, we incubated **4a**–**r** with rat plasma over 72 h. The results gave direct evidence on the important role of the alkyl chain linker. The *in vitro* half-lives of conjugates with a C2 or C5 alkyl chain linker were only moderately improved, while the half-lives of conjugates with a C11 alkyl chain linker were as long as liraglutide. Next, in order to further increase the albumin binding affinity of selected conjugates (**4c**, **4i**, **4r**) to explore the possibility for further improvement of their stabilities, two O2Oc spacers were introduced between the peptides and LCA in an attempt to optimize their LCA side chains, affording **5a**–**c**. To quantify the impact of the O2Oc spacer on the potency of **5a**–**c**, their *in vivo* glucose-lowering activities were evaluated. The results showed that the O2Oc linker was well tolerated by **4c**, **4i** and **4r**, and only **5a** showed a slightly decreased hypoglycemic activity. Importantly, the *in vitro* stabilities of **5a**–**c** were significantly enhanced, which may be attributed to the increased albumin binding affinity.

The HSA affinity of the selected compound **5b** was studied by HPAC analysis and compared with **4i**, liraglutide and semaglutide. As expected, **5b** displayed an increased albumin binding affinity relative to the native peptide **4i** and liraglutide. However, the albumin binding affinity of **5b** was still lower than semaglutide. The possible reason is the relatively short alkyl chain and the absence of acidic groups, both of which were proved to be important for the extremely high albumin affinity of semaglutide.[13, 20] Subsequent pharmacokinetic studies revealed that **5b** had a circulation half-life two-fold longer than that of **4i**, which is consistent with the higher albumin binding affinity of **5b**. Furthermore, **5b** exhibited comparable hypoglycemic and insulinotropic activities in *db/db* mice to liraglutide and semaglutide, indicating the potent biological activities of **5b** *in vivo*. The hypoglycemic duration of **5b** was much greater than that of liraglutide, and further dose-response study revealed that **5b** had a dose-dependent anti-diabetic efficacy and could potently lower blood glucose concentrations for at least 24 h (25 nmol·kg^{-1}) or 48 h (150 nmol·kg^{-1}). However, the anti-diabetic duration of **5b** was still lower than that of semaglutide, which could lower blood glucose concentrations for at least 48 h. It could be speculated that the N-terminal Aib_2-Glu_3 region of semaglutide is more resistant to DPP-IV cleavage than the Gly_2-Glu_3 in **5b**. This might account for the shorter anti-diabetic duration of **5b** *in vivo* than semaglutide. During the hypoglycemic duration tests, the inhibitory effect of **5b** on food intake was also investigated. Liraglutide, semaglutide and **5b** exhibited potent effects on food intake during 0–12 h, while these effects were evidently different at 24 h. These differences in anorectic effects among liraglutide, semaglutide and **5b** may presumably be attributed to their different pharmacokinetics.

The preliminary toxicity tests of **5b** demonstrated its low *in vitro* toxicity and *in vivo* hepatoxicity. Normally, the toxicity of LCA is evident in mice when the administered dose exceeds 100

mg/kg/day,[42] which is much larger that the tested dose of **5b** in acute toxicity test (100 mg·kg^{-1} of LCA corresponds to ~1395 mg·kg^{-1} of **5b**) and the administration dose of **5b** in other biological tests (~0.14–0.79 mg·kg^{-1}). However, further chronic toxicity test of **5b** still needs to be performed to more precisely evaluate the toxicity of **5b**. A once daily injection of **5b** showed prominent hypoglycemic effects associated with promotion of insulin secretion in *db/db* mice. Similar to liraglutide, chronic administration of **5b** prohibited the worsening of the HbA1c and improved glucose tolerance. The immunohistochemistry further proved that the enhanced glucose tolerance effect of **5b** was attributed to the beneficial effect of **5b** on amelioration of pancreatic endocrine deficiencies. The biochemical analysis results revealed that **5b** did not show significant hepatic toxicity after the five-week treatment. Overall, these beneficial preclinical data of **5b** indicate the potential of **5b** as a long-acting hypoglycemic agent.

In summary, we report the synthesis and SAR of a series of *Xenopus* GLP-1 analogues derivatized with LCA on the amine of Lys with the aim to discover novel long-acting GLP-1 receptor agonists for the treatment of T2DM. Our studies identified **5b** with a half-life of 11.0 h in rats after *s.c.* dosing as well as similar *in vivo* glucose-lowering activity to liraglutide and semaglutide. Hypoglycemic duration study of **5b** in non-fasted *db/db* mice demonstrated a duration of **5b** > 24 h at a dose of 25 nmol·kg^{-1}. In *db/db* mice, daily administration of **5b** achieved beneficial effects on HbA1c, food intake, body weight and blood glucose. Importantly, insulin immunostaining revealed the treatment effects of **5b** on islet of *db/db* mice. The preclinical results of **5b** suggest that it has a promising therapeutic potential as a novel long-acting GLP-1 receptor agonist. Further structure modifications based on the current results may further improve the therapeutic efficacy and stability of **5b**.

Supporting Information

Characterization of **4a**–**4r** and **5a**–**5c**.

Notes

The authors declare that no competing financial interests.

ORCID ID

Jing Han: 0000-0001-5605-1868

Junjie Fu: 0000-0002-2741-7469

Author contributions

Jing Han designed the research study. Jing Han, Liming Zhao, Ying Zhang, Xinyu Chen, Lidan Sun, Junjie Fu, Feng Zhou and Yingying Fei performed the research. Jing Han and Junjie Fu analyzed the data and wrote the paper.

Acknowledgment

This work is supported by the National Natural Science Foundation of China (Nos. 81602964, 81602960 and 81703346), the Natural Science Foundation of Jiangsu Province (Grants No BK20150243 and BK20161028), the Science and Technology Support Program of Jiangsu Province (No. BE2017643), PAPD of Jiangsu Higher Education Institutions, and the Jiangsu Overseas Visiting Scholar Program for University Prominent Young & Middle-aged Teachers and Presidents.

Abbreviations:

AUC, area under the curve; ALT, alanine aminotransferase; AST, aspartate aminotransferase; cAMP, cyclic adenosine monophosphate; CA, cholic acid; CDCA, chenodeoxycholic acid; DCA, deoxycholic acid; GLP-1, glucagon-like peptide-1; HSA, human serum albumin; HPAC, high performance affinity chromatography; HTRF, homogeneous time-resolved fluorescence technology; IPGTT, intraperitoneal glucose tolerance testing; IOD, integrated optical density; LCA, lithocholic acid; LC-MS/MS, liquid chromatography-tandem mass spectrometry; MPA, mycophenolic acid; SAR, structure-activity relationships; SPPS, solid-phase peptide synthesis; T2DM, type 2 diabetes mellitus

References

1. Meier, J. J. GLP-1 receptor agonists for individualized treatment of type 2 diabetes mellitus. *Nat. Rev. Endocrinol.* **2012**, 8, 728-742.

2. Zhou, J.; Cai, X.; Huang, X.; Dai, Y.; Sun, L.; Zhang, B.; Yang, B.; Lin, H.; Huang, W.; Qian, H. A novel glucagon-like peptide-1/glucagon receptor dual agonist exhibits weight-lowering and diabetes-protective effects. *Eur. J. Med. Chem.* **2017**, 138, 1158-1169.

3. Kim, M.; Platt, M. J.; Shibasaki, T.; Quaggin, S. E.; Backx, P. H.; Seino, S.; Simpson, J. A.; Drucker, D. J. GLP-1 receptor activation and Epac2 link atrial natriuretic peptide secretion to control of blood pressure. *Nat. Med.* **2013**, 19, 567-575.

4. Tschöp, M. H.; Finan, B.; Clemmensen, C.; Gelfanov, V.; Perez-Tilve, D.; Müller, T. D.; DiMarchi, R. D. Unimolecular polypharmacy for treatment of diabetes and obesity. *Cell Metab.* **2016**, 24, 51-62.

5. Steele, A. M.; Shields, B. M.; Wensley, K. J.; Colclough, K.; Ellard, S.; Hattersley, A. T. Prevalence of vascular complications among patients with glucokinase mutations and prolonged, mild hyperglycemia. *JAMA* **2014**, 311, 279-286.

6. Sun, Y.-M.; Su, Y.; Li, J.; Wang, L.-F. Recent advances in understanding the biochemical and molecular mechanism of diabetic nephropathy. *Biochem. Biophys. Res. Commun.* **2013**, 433, 359-361.

7. Son, S.; Chae, S. Y.; Kim, C. W.; Choi, Y. G.; Jung, S. Y.; Lee, S.; Lee, K. C. Preparation and structural, biochemical, and pharmaceutical characterizations of bile acid-modified long-acting exendin-4 derivatives. *J. Med. Chem.* **2009**, 52, 6889-6896.

8. Day, J. W.; Ottaway, N.; Patterson, J. T.; Gelfanov, V.; Smiley, D.; Gidda, J.; Findeisen, H.; Bruemmer, D.; Drucker, D. J.; Chaudhary, N. A new glucagon and GLP-1 co-agonist eliminates obesity in rodents. *Nat. Chem. Biol.* **2009**, 5, 749-757.

9. Mapelli, C.; Natarajan, S. I.; Meyer, J.-P.; Bastos, M. M.; Bernatowicz, M. S.; Lee, V. G.; Pluscec, J.; Riexinger, D. J.; Sieber-McMaster, E. S.; Constantine, K. L. Eleven amino acid glucagon-like peptide-1 receptor agonists with antidiabetic activity. *J. Med. Chem.* **2009**, 52, 7788-7799.

10. Bech, E. M.; Martos-Maldonado, M. C.; Wismann, P.; Sørensen, K. K.; van Witteloostuijn, S. B.; Thygesen, M. B.; Vrang, N.; Jelsing, J.; Pedersen, S. L.; Jensen, K. J. Peptide Half-Life

Extension: Divalent, Small-Molecule Albumin Interactions Direct the Systemic Properties of Glucagon-Like Peptide 1 (GLP-1) Analogues. *J. Med. Chem.* **2017**, 60, 7434-7446.

11. Miranda, L. P.; Winters, K. A.; Gegg, C. V.; Patel, A.; Aral, J.; Long, J.; Zhang, J.; Diamond, S.; Guido, M.; Stanislaus, S. Design and synthesis of conformationally constrained glucagon-like peptide-1 derivatives with increased plasma stability and prolonged in vivo activity. *J. Med. Chem.* **2008**, 51, 2758-2765.

12. Finan, B.; Clemmensen, C.; Müller, T. D. Emerging opportunities for the treatment of metabolic diseases: glucagon-like peptide-1 based multi-agonists. *Mol. Cell. Endocrinol.* **2015**, 418, 42-54.

13. Lau, J.; Bloch, P.; Schäffer, L.; Pettersson, I.; Spetzler, J.; Kofoed, J.; Madsen, K.; Knudsen, L. B.; McGuire, J.; Steensgaard, D. B. Discovery of the once-weekly glucagon-like peptide-1 (GLP-1) analogue semaglutide. *J. Med. Chem.* **2015**, 58, 7370-7380.

14. Evers, A.; Haack, T.; Lorenz, M.; Bossart, M.; Elvert, R.; Henkel, B.; Stengelin, S.; Kurz, M.; Glien, M.; Dudda, A. Design of Novel Exendin-Based Dual Glucagon-like Peptide 1 (GLP-1)/Glucagon Receptor Agonists. *J. Med. Chem.* **2017**, 60, 4293-4303.

15. Cantini, G.; Mannucci, E.; Luconi, M. Perspectives in GLP-1 research: new targets, new receptors. *Trends Endocrin. Met.* **2016**, 27, 427-438.

16. Irwin, D. M.; Satkunarajah, M.; Wen, Y.; Brubaker, P. L.; Pederson, R. A.; Wheeler, M. B. The Xenopus proglucagon gene encodes novel GLP-1-like peptides with insulinotropic properties. *Proc. Natl. Acad. Sci. U. S. A.* **1997**, 94, 7915-7920.

17. Han, J.; Wang, Y.; Meng, Q.; Li, G.; Huang, F.; Wu, S.; Fei, Y.; Zhou, F.; Fu, J. Design, synthesis and biological evaluation of PEGylated Xenopus glucagon-like peptide-1 derivatives as long-acting hypoglycemic agents. *Eur. J. Med. Chem.* **2017**, 132, 81-89.

18. Han, J.; Chen, X.; Wang, Y.; Fei, Y.; Zhou, F.; Zhang, Y.; Liu, L.; Si, P.; Fu, J. Xenopus GLP-1-inspired discovery of novel GLP-1 receptor agonists as long-acting hypoglycemic and insulinotropic agents with significant therapeutic potential. *Biochem. Pharmacol.* **2017**, 142, 155-167.

19. Han, J.; Fei, Y.; Zhou, F.; Chen, X.; Zhang, Y.; Liu, L.; Fu, J. Xenopus-derived glucagon-like peptide-1 and polyethylene-glycosylated glucagon-like peptide-1 receptor agonists: long-acting hypoglycaemic and insulinotropic activities with potential therapeutic utilities. *Br. J. Pharmacol.* **2018**, 175, 544-557.

20. Madsen, K.; Knudsen, L. B.; Agersoe, H.; Nielsen, P. F.; Thøgersen, H.; Wilken, M.; Johansen, N. L. Structure-activity and protraction relationship of long-acting glucagon-like peptide-1 derivatives: importance of fatty acid length, polarity, and bulkiness. *J. Med. Chem.* **2007**, 50, 6126-6132.

21. Bellmann-Sickert, K.; Elling, C. E.; Madsen, A. N.; Little, P. B.; Lundgren, K.; Gerlach, L.-O.; Bergmann, R.; Holst, B.; Schwartz, T. W.; Beck-Sickinger, A. G. Long-acting lipidated analogue of human pancreatic polypeptide is slowly released into circulation. *J. Med. Chem.* **2011**, 54, 2658-2667.

22. Katsuma, S.; Hirasawa, A.; Tsujimoto, G. Bile acids promote glucagon-like peptide-1 secretion through TGR5 in a murine enteroendocrine cell line STC-1. *Biochem. Biophys. Res. Commun.* **2005**, 329, 386-390.

23. Staels, B.; Kuipers, F. Bile acid sequestrants and the treatment of type 2 diabetes mellitus. *Drugs* **2007**, 67, 1383-1392.

24. Aldini, R.; Roda, A.; Labate, A. M.; Cappelleri, G.; Roda, E.; Barbara, L. Hepatic bile acid uptake: effect of conjugation, hydroxyl and keto groups, and albumin binding. *J. Lipid Res.* **1982**, 23, 1167-1173.

25. Roda, A.; Cappelleri, G.; Aldini, R.; Roda, E.; Barbara, L. Quantitative aspects of the interaction of bile acids with human serum albumin. *J. Lipid Res.* **1982**, 23, 490-495.

26. Han, J.; Fu, J.; Sun, L.; Han, Y.; Mao, Q.; Liao, F.; Zheng, X.; Zhu, K. Synthesis and pharmaceutical characterization of site specific mycophenolic acid-modified Xenopus glucagon-like peptide-1 analogs. *Med. Chem. Commun.* **2018**, 9, 67-80.

27. Han, J.; Fei, Y.; Zhou, F.; Chen, X.; Zheng, W.; Fu, J. Micellar Nanomedicine of Novel Fatty Acid Modified Xenopus Glucagon-like Peptide-1: Improved Physicochemical Characteristics and Therapeutic Utilities for Type 2 Diabetes. *Mol. Pharmaceut.* **2017**, 14, 3954-3967.

28. Han, J.; Sun, L.; Huang, X.; Li, Z.; Zhang, C.; Qian, H.; Huang, W. Novel coumarin modified GLP-1 derivatives with enhanced plasma stability and prolonged in vivo glucose-lowering ability. *Br. J. Pharmacol.* **2014**, 171, 5252-5264.

29. Han, J.; Huang, X.; Sun, L.; Li, Z.; Qian, H.; Huang, W. Novel fatty chain-modified glucagon-like peptide-1 conjugates with enhanced stability and prolonged in vivo activity. *Biochem. Pharmacol.* **2013**, 86, 297-308.

30. Singh, S. S.; Mehta, J. Measurement of drug–protein binding by immobilized human serum albumin-HPLC and comparison with ultrafiltration. *J. Chromatogr. B* **2006**, 834, 108-116.

31. Cui, X.; Meng, Q.; Chu, Y.; Gu, X.; Tang, Y.; Zhou, F.; Fei, Y.; Fu, J.; Han, J. Glucagon-like peptide-1 loaded phospholipid micelles for the treatment of type 2 diabetes: improved pharmacokinetic behaviours and prolonged glucose-lowering effects. *RSC Adv.* **2016**, 6, 94408-94416.

32. Kim, T. H.; Jiang, H. H.; Lee, S.; Youn, Y. S.; Park, C. W.; Byun, Y.; Chen, X.; Lee, K. C. Mono-PEGylated dimeric exendin-4 as high receptor binding and long-acting conjugates for type 2 anti-diabetes therapeutics. *Bioconjugate Chem.* **2011**, 22, 625-632.

33. Han, J.; Zhou, F.; Fei, Y.; Chen, X.; Fu, J.; Qian, H. Preparation and Pharmaceutical Characterizations of Lipidated Dimeric Xenopus Glucagon-like Peptide-1 Conjugates. *Bioconjugate Chem.* **2018**, 29, 390-402.

34. Yang, B.; Li, X.; Zhang, C.; Yan, S.; Wei, W.; Wang, X.; Deng, X.; Qian, H.; Lin, H.; Huang, W. Design, synthesis and biological evaluation of novel peptide MC2 analogues from Momordica charantia as potential anti-diabetic agents. *Org. Biomol. Chem.* **2015**, 13, 4551-4561.

35. Doyle, M. E.; Theodorakis, M. J.; Holloway, H. W.; Bernier, M.; Greig, N. H.; Egan, J. M. The importance of the nine-amino acid C-terminal sequence of exendin-4 for binding to the GLP-1 receptor and for biological activity. *Regul. Peptides* **2003**, 114, 153-158.

36. Werner, U.; Haschke, G.; Herling, A. W.; Kramer, W. Pharmacological profile of lixisenatide: A new GLP-1 receptor agonist for the treatment of type 2 diabetes. *Regul. Peptides* **2010**, 164, 58-64.

37. Han, J.; Sun, L.; Chu, Y.; Li, Z.; Huang, D.; Zhu, X.; Qian, H.; Huang, W. Design, synthesis, and biological activity of novel dicoumarol glucagon-like peptide 1 conjugates. *J. Med. Chem.* **2013**, 56, 9955-9968.

38. Bolli, G.; Owens, D. Lixisenatide, a novel GLP-1 receptor agonist: efficacy, safety and clinical implications for type 2 diabetes mellitus. *Diabetes Obes. Metab.* **2014**, 16, 588-601.

39. Lee, J. G.; Ryu, J. H.; Kim, S.-M.; Park, M.-Y.; Kim, S.-H.; Shin, Y. G.; Sohn, J.-W.; Kim, H. H.; Park, Z.-Y.; Seong, J. Y. Replacement of the C-terminal Trp-cage of Exendin-4 with a Fatty Acid Improves Therapeutic Utility. *Biochem. Pharmacol.* **2018**, 151, 59-68.

40. Beeken, W. L.; Volwiler, W.; Goldsworthy, P. D.; Garby, L. E.; Reynolds, W. E.; Stogsdill, R.; Stemler, R. S. Studies of I^{131}-albumin catabolism and distribution in normal young male adults. *J. Clin. Invest.* **1962**, 41, 1312-1333.

41. van Witteloostuijn, S. B.; Mannerstedt, K.; Wismann, P.; Bech, E. M.; Thygesen, M. B.; Vrang, N.; Jelsing, J.; Jensen, K. J.; Pedersen, S. L. Neoglycolipids for Prolonging the Effects of Peptides: Self-Assembling Glucagon-like Peptide 1 Analogues with Albumin Binding Properties and Potent in Vivo Efficacy. *Mol. Pharmaceut.* **2016**, 14, 193-205.

42. Kitada, H.; Miyata, M.; Nakamura, T.; Tozawa, A.; Honma, W.; Shimada, M.; Nagata, K.; Sinal, C. J.; Guo, G. L.; Gonzalez, F. J. Protective role of hydroxysteroid sulfotransferase in lithocholic acid-induced liver toxicity. *J. Bio. Chem.* **2003**, 278, 17838-17844.

Scheme 1. Synthetic route of **4a**–**r**. PG: Acid labile protecting group.

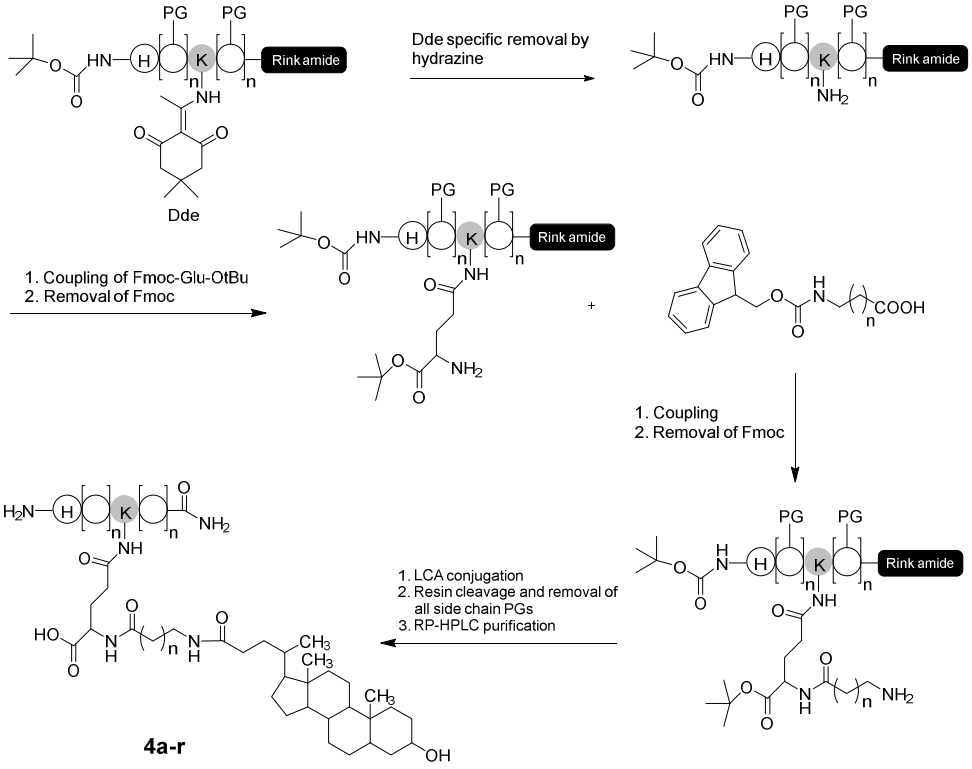

Scheme 2. Synthetic route of **5a–c**. PG: Acid labile protecting group.

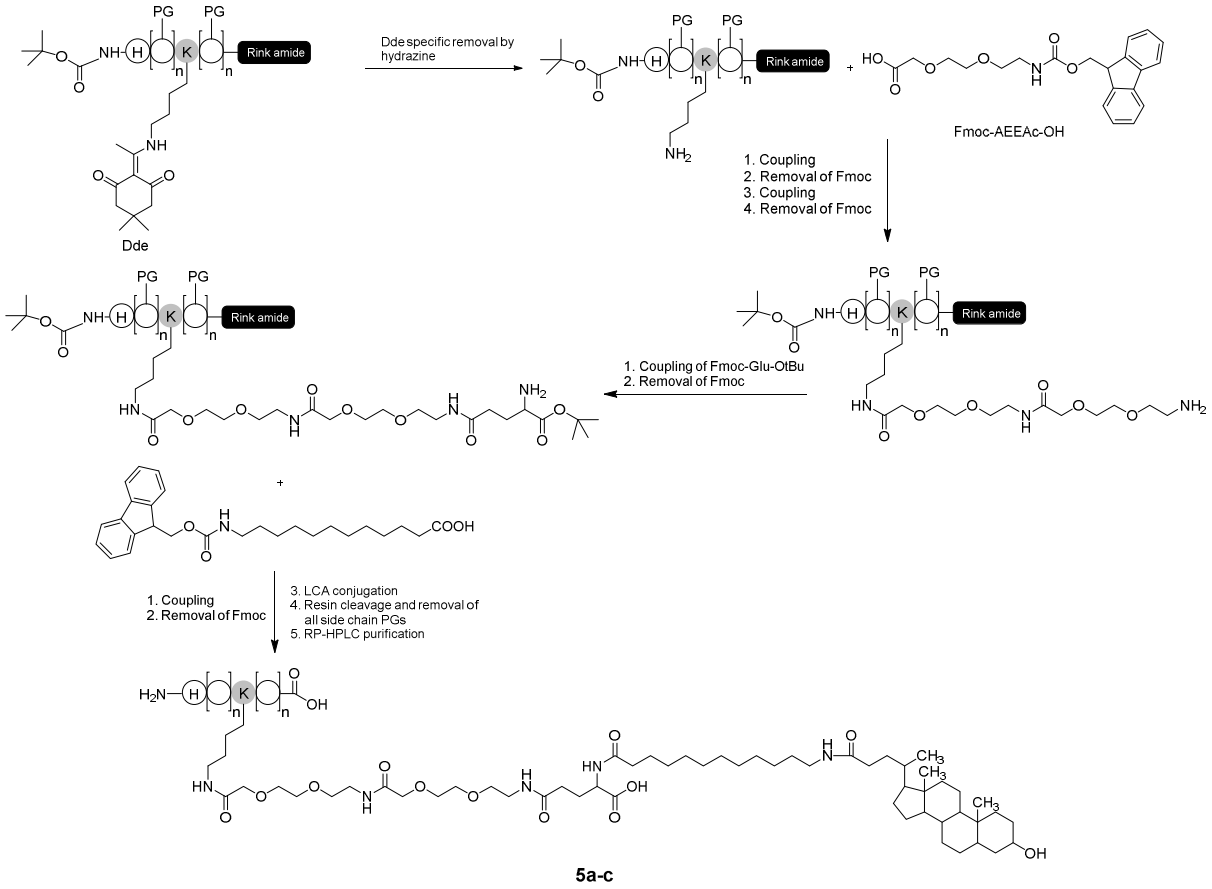

Table 1. The *in vitro* and *in vivo* bioactivities of **4a**−**r**

Compounds	EC_{50} (nM)[a]	$AUC_{glucose\ 0\text{-}120min}$[b]	Compounds	EC_{50} (nM)[a]	$AUC_{glucose\ 0\text{-}120min}$[b]
GLP-1	0.41 ± 0.07	817 ± 81	**4h**	0.57 ± 0.19	682 ± 33***
1	0.32 ± 0.09	702 ± 57*	**4i**	0.88 ± 0.43	859 ± 66
2	0.21 ± 0.03	622 ± 27***	**4j**	0.31 ± 0.03	638 ± 33***
3	0.12 ± 0.08	556 ± 51***	**4k**	0.68 ± 0.24	853 ± 38
4a	0.29 ± 0.04	694 ± 40*	**4l**	2.09 ± 0.21	938 ± 27
4b	0.97 ± 0.11	753 ± 31	**4m**	0.18 ± 0.06	478 ± 18***
4c	1.49 ± 0.13	882 ± 50	**4n**	0.44 ± 0.11	541 ± 21***
4d	0.49 ± 0.07	803 ± 66	**4o**	0.98 ± 0.18	774 ± 36
4e	1.68 ± 0.18	936 ± 27	**4p**	0.14 ± 0.02	421 ± 15***
4f	6.35 ± 0.39	1037 ± 74	**4q**	0.48 ± 0.08	563 ± 8***
4g	0.18 ± 0.02	540 ± 20***	**4r**	0.61 ± 0.24	567 ± 45***

[a]Data are represented as EC_{50}. Values are the means ± SD of three individual experiments and repeated three times (n = 3).

[b]$AUC_{glucose}$ values were calculated by IPGTT in Kunming mice. Means ± SD, n = 6. *P < 0.05 vs. GLP-1, ***P < 0.001 vs. GLP-1.

Table 2. The *in vitro* plasma stabilities of **4a**−**r**

Compounds	Plasma half-life (h)	Compounds	Plasma half-life (h)
Liraglutide	35.4	**4j**	24.1
4a	17.4	**4k**	30.1
4b	27.7	**4l**	40.5
4c	37.7	**4m**	18.8
4d	20.2	**4n**	26.6
4e	29.4	**4o**	36.4
4f	37.3	**4p**	16.9
4g	21.5	**4q**	27.2
4h	31.6	**4r**	38.7
4i	39.5		

Table 3. Effects of the liraglutide and **5b** on AST and ALT levels after chronic treatment.

Group	AST[a] ($IU \cdot L^{-1}$)	ALT[a] ($IU \cdot L^{-1}$)
Saline	80.6 ± 9.1	28.2 ± 4.9
Liraglutide	88.2 ± 4.9	24.5 ± 8.1
5b	76.9 ± 10.2	32.9 ± 7.3

[a]Data are means ± SD (n = 6).

Figure legends

Figure 1. Structures of GLP-1, exendin-4, lixisenatide, peptides **1**–**3** and conjugates **4a**–**r**.

Figure 2. Concentration response curves of GLP-1 and representative LCA-*Xenopus* GLP-1 conjugates in receptor activation. The data for the test compounds were normalized and plotted as the percentage of maximum cAMP levels stimulated by saturating GLP-1. All experiments were carried out in triplicate and repeated three times (n = 3). Means ± SD.

Figure 3. Acute hypoglycemic effects of GLP-1 and **4a**–**r** in Kunming mice. GLP-1 and **4a**–**r** (25 nmol·kg^{-1}) were *i.p.* loaded at -10 min, followed by *i.p.* glucose loaded (2 g·kg^{-1}) at 0 min. (A-D) Time-response curves of blood glucose concentrations in each group. Means ± SD, n = 6.

Figure 4. Degradation of liraglutide and **4a**–**r** in rat plasma. Means ± SD, n = 3.

Figure 5. Structures of **5a**–**c**.

Figure 6. Stability and biological activity tests of **5a**–**c**. (A) Degradation of liraglutide and **5a**–**c** in rat plasma. Means ± SD, n = 3. (B) Concentration response curves of liraglutide and **5a**–**c** in receptor activation. The data for the test compounds were normalized and plotted as the percentage of maximum cAMP levels stimulated by saturating GLP-1. Means ± SD. Experiments were performed in triplicate and repeated three times (n = 3). (C) Time-response curves of blood glucose in liraglutide and **5a**–**c** groups. (D) $AUC_{glucose\ 0\text{-}120\ min}$ after *i.p.* glucose administration. Means ± SD, n = 6.

Figure 7. Physicochemical and pharmacokinetic profiles of **5b**. (A) The albumin binding affinities of liraglutide, semaglutide, **4i** and **5b** were measured on HSA HPLC column (*k*'). (B) Pharmacokinetic profiles of **4i** and **5b** after *s.c.* administration in SD rat (50 nmol·kg^{-1}). Means ± SD, n = 3.

Figure 8. Glucose-lowering and insulinotropic activities of liraglutide, semaglutide and **5b** (25 nmol·kg^{-1}, *i.p.*) tested by IPGTT in *db/db* mice. (A) The course of blood glucose concentrations in each group. (B) $AUC_{glucose\ 0\text{-}180\ min}$ after *i.p.* glucose administration. (C) Plasma insulin levels in each group of *db/db* mice at 10, 15 and 20 min post *i.p.* glucose load. Means ± SD, n = 6. $^{***}P < 0.001$ *vs.* Saline.

Figure 9. Dose response studies for the hypoglycemic efficacies of liraglutide, semaglutide and **5b** in nonfasted *db/db* mice after *i.p.* dosing of 25 or 150 nmol·kg^{-1}. (A and C) Plots of blood glucose levels of liraglutide, semaglutide and **5b** at the dose of 25 nmol·kg^{-1} (A) or 150 nmol·kg^{-1} (C). (B and D) Calculated glucose $AUC_{0\text{-}60\ h}$ values in each group of mice. Means ± SD, n = 6. $^{*}P < 0.05$ *vs.* Saline, $^{***}P < 0.001$ *vs.* Saline. $^{b}P < 0.01$ *vs.* Liraglutide. $^{c}P < 0.001$ *vs.* Liraglutide.

Figure 10. Anorectic and toxicity tests of **5b**. (A) Cumulated food intake (0–24 h) of liraglutide, semaglutide and **5b** (25 nmol·kg^{-1}) in hypoglycemic efficacy tests. Means ± SD, n = 6. (B) Effects of liraglutide, semaglutide (10 nM), and **5b** (10, 100, and 1000 nM) on the viability of INS-1 cells. (C) Acute *in vivo* toxicity of **5b** (100 or 500 mg·kg^{-1}, dosing 2 days) in *db/db* mice. Means ± SD, n = 3.

Figure 11. Effects of liraglutide and **5b** on *db/db* mice during a five-week treatment. (A) HbA1c (%) values in each group as measured weekly. (B) Food intake amount (g/mouse). (C) Body weight change (g/mouse). (D) Non-fasting blood glucose concentrations as measured every two days. (E) Non-fasting insulin concentrations as measured every week. (F) IPGTT test performed after the treatment period. Means ± SD, n = 6.

Figure 12. Immunohistochemistry analysis of pancreatic tissue sections in *db/db* mice after five weeks of study. Representative images of insulin immunostaining sections in saline (A), liraglutide

(B) and **5b** (C) groups. (D) Integrated optical density (IOD) values of insulin in each group. Data are represented as the Means ± SD for six mice per group.

GLP-1	HAEGT FTSDV SSYLE GQAAK EFIAW LVKGR
Exendin-4	HGEGT FTSDL SKQME EEAVR LFIEW LKNGG PSSGA PPPS
Lixisenatide	HGEGT FTSDL SKQME EEAVR LFIEW LKNGG PSSGA PPSKK KKKK
1	HGEGT YTNDV TEYLE EEAAK EFIEW LIKGK
2	HGEGT YTNDV TEYLE EEAAK EFIEW LIKGK PSSGA PPPS
3	HGEGT YTNDV TEYLE EEAAK EFIEW LIKGK PSSGA PPSKK KKKK
4a	HGEGT YTNDV TEYLE EEAAX_1 EFIEW LIKGK
4b	HGEGT YTNDV TEYLE EEAAX_2 EFIEW LIKGK
4c	HGEGT YTNDV TEYLE EEAAX_3 EFIEW LIKGK
4d	HGEGT YTNDV TEYLE EEAAK EFIEW LIX_1GK
4e	HGEGT YTNDV TEYLE EEAAK EFIEW LIX_2GK
4f	HGEGT YTNDV TEYLE EEAAK EFIEW LIX_3GK
4g	HGEGT YTNDV TEYLE EEAAX_1 EFIEW LIKGK PSSGA PPPS
4h	HGEGT YTNDV TEYLE EEAAX_2 EFIEW LIKGK PSSGA PPPS
4i	HGEGT YTNDV TEYLE EEAAX_3 EFIEW LIKGK PSSGA PPPS
4j	HGEGT YTNDV TEYLE EEAAK EFIEW LIX_1GK PSSGA PPPS
4k	HGEGT YTNDV TEYLE EEAAK EFIEW LIX_2GK PSSGA PPPS
4l	HGEGT YTNDV TEYLE EEAAK EFIEW LIX_3GK PSSGA PPPS
4m	HGEGT YTNDV TEYLE EEAAX_1 EFIEW LIKGK PSSGA PPSKK KKKK
4n	HGEGT YTNDV TEYLE EEAAX_2 EFIEW LIKGK PSSGA PPSKK KKKK
4o	HGEGT YTNDV TEYLE EEAAX_3 EFIEW LIKGK PSSGA PPSKK KKKK
4p	HGEGT YTNDV TEYLE EEAAK EFIEW LIX_1GK PSSGA PPSKK KKKK
4q	HGEGT YTNDV TEYLE EEAAK EFIEW LIX_2GK PSSGA PPSKK KKKK
4r	HGEGT YTNDV TEYLE EEAAK EFIEW LIX_3GK PSSGA PPSKK KKKK

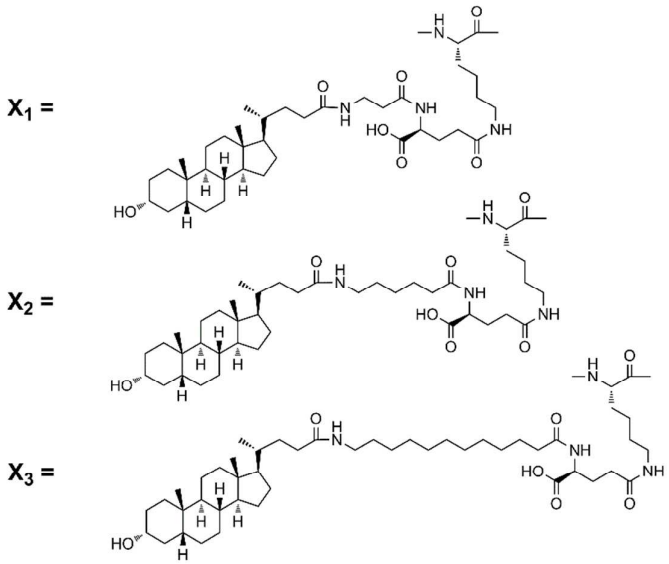

Figure 1. Structures of GLP-1, exendin-4, lixisenatide, peptides **1**–**3** and conjugates **4a**–**r**.

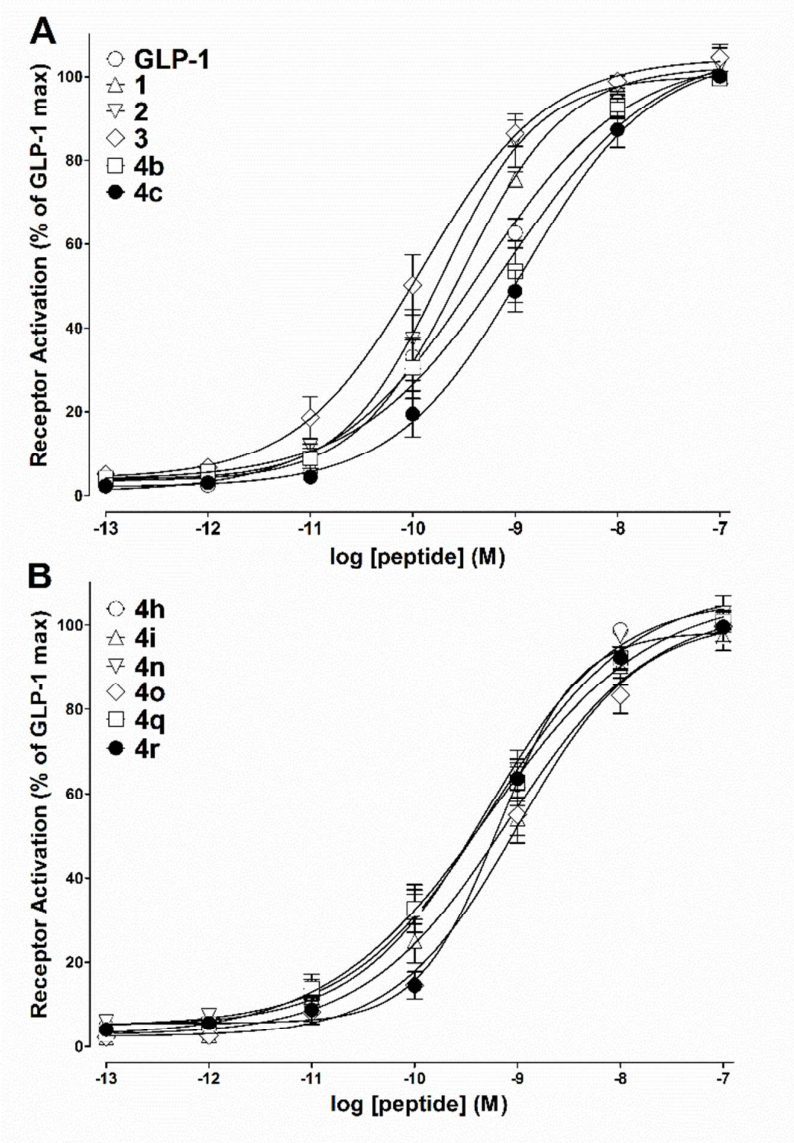

Figure 2. Concentration response curves of GLP-1 and representative LCA-*Xenopus* GLP-1 conjugates in receptor activation. The data for the test compounds were normalized and plotted as the percentage of maximum cAMP levels stimulated by saturated GLP-1. All experiments were carried out in triplicate and repeated three times (n = 3). Means ± SD.

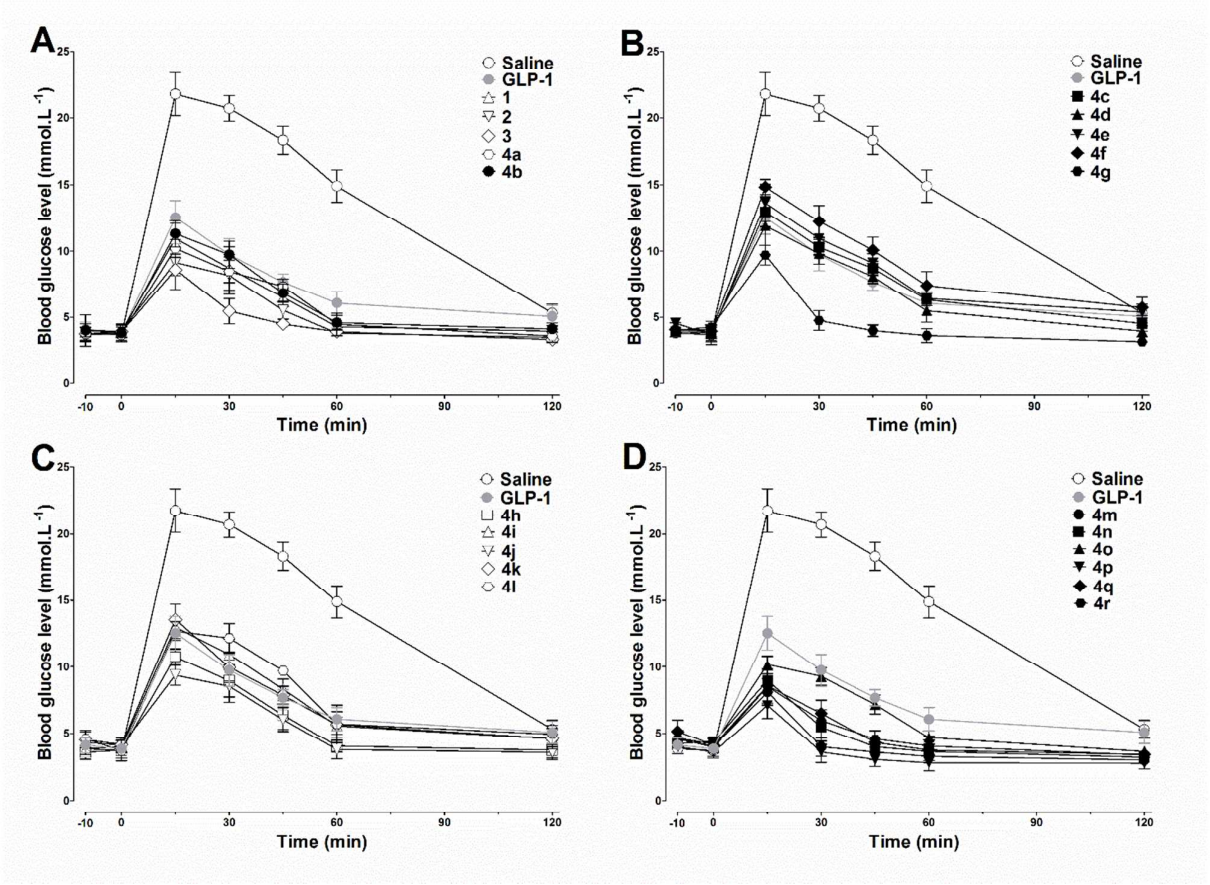

Figure 3. Acute hypoglycemic effects of GLP-1 and **4a**–**r** in Kunming mice. GLP-1 and **4a**–**r** (25 nmol·kg^{-1}) were *i.p.* loaded at -10 min, followed by *i.p.* glucose loaded (2 g·kg^{-1}) at 0 min. (A-D) Time-response curves of blood glucose concentrations in each group. Means ± SD, n = 6.

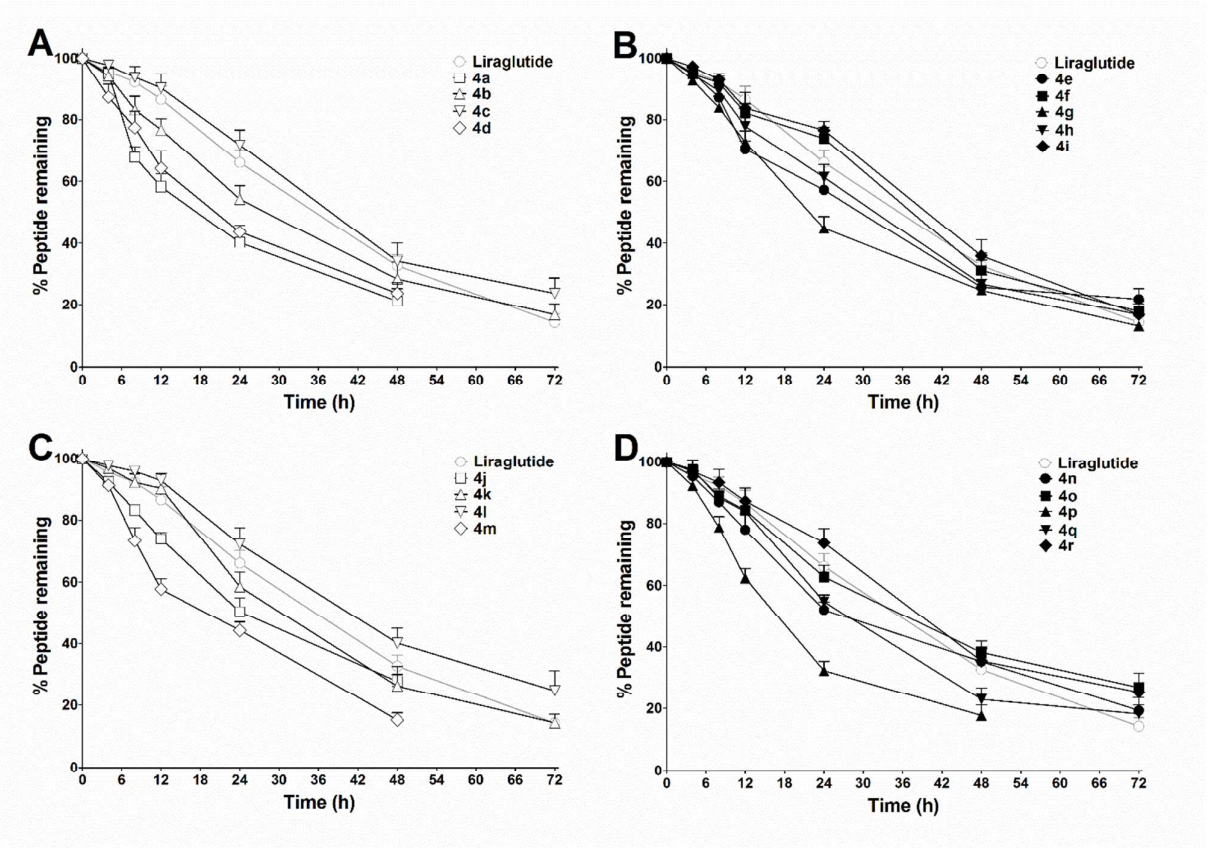

Figure 4. Degradation of liraglutide and **4a**–**r** in rat plasma. Means ± SD, n = 3.

5a HGEGT YTNDV TEYLE EEAAX_4 EFIEW LIKGK

5b HGEGT YTNDV TEYLE EEAAX_4 EFIEW LIKGK PSSGA PPPS

5c HGEGT YTNDV TEYLE EEAAK EFIEW LIX_4GK PSSGA PPSKK KKKK

X_4 =

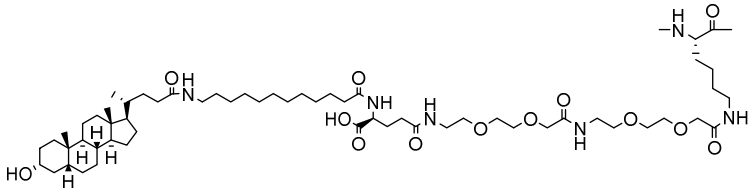

Figure 5. Structures of **5a**–**c**.

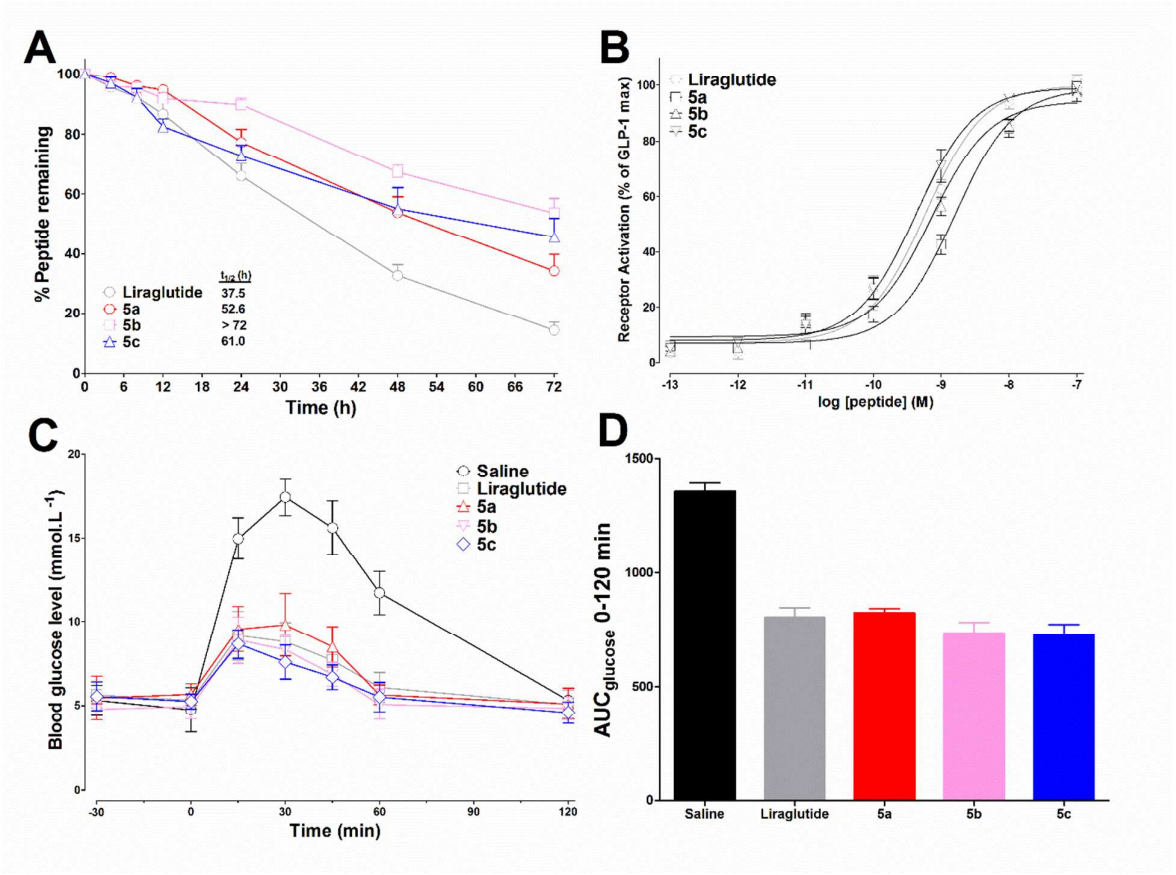

Figure 6. Stability and biological activity tests of **5a–c**. (A) Degradation of liraglutide and **5a–c** in rat plasma. Means ± SD, n = 3. (B) Concentration response curves of liraglutide and **5a–c** in receptor activation. The data for the test compounds were normalized and plotted as the percentage of maximum cAMP levels stimulated by saturated GLP-1. Means ± SD. Experiments were performed in triplicate and repeated three times (n = 3). (C) Time-response curves of blood glucose in liraglutide and **5a–c** groups. (D) $AUC_{glucose\ 0\text{-}120\ min}$ after *i.p.* glucose administration. Means ± SD, n = 6.

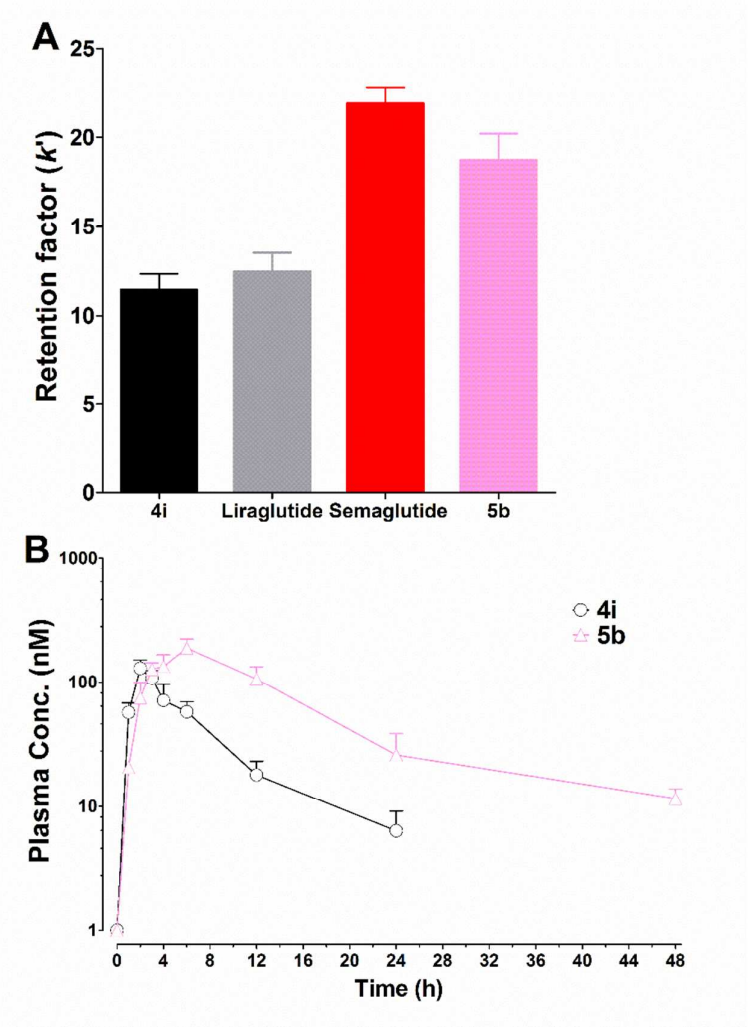

Figure 7. Physicochemical and pharmacokinetic profiles of **5b**. (A) The albumin binding affinities of liraglutide, semaglutide, **4i** and **5b** were measured on HSA HPLC column (*k*'). (B) Pharmacokinetic profiles of **4i** and **5b** after *s.c.* administration in SD rat (50 nmol·kg^{-1}). Means ± SD, n = 3.

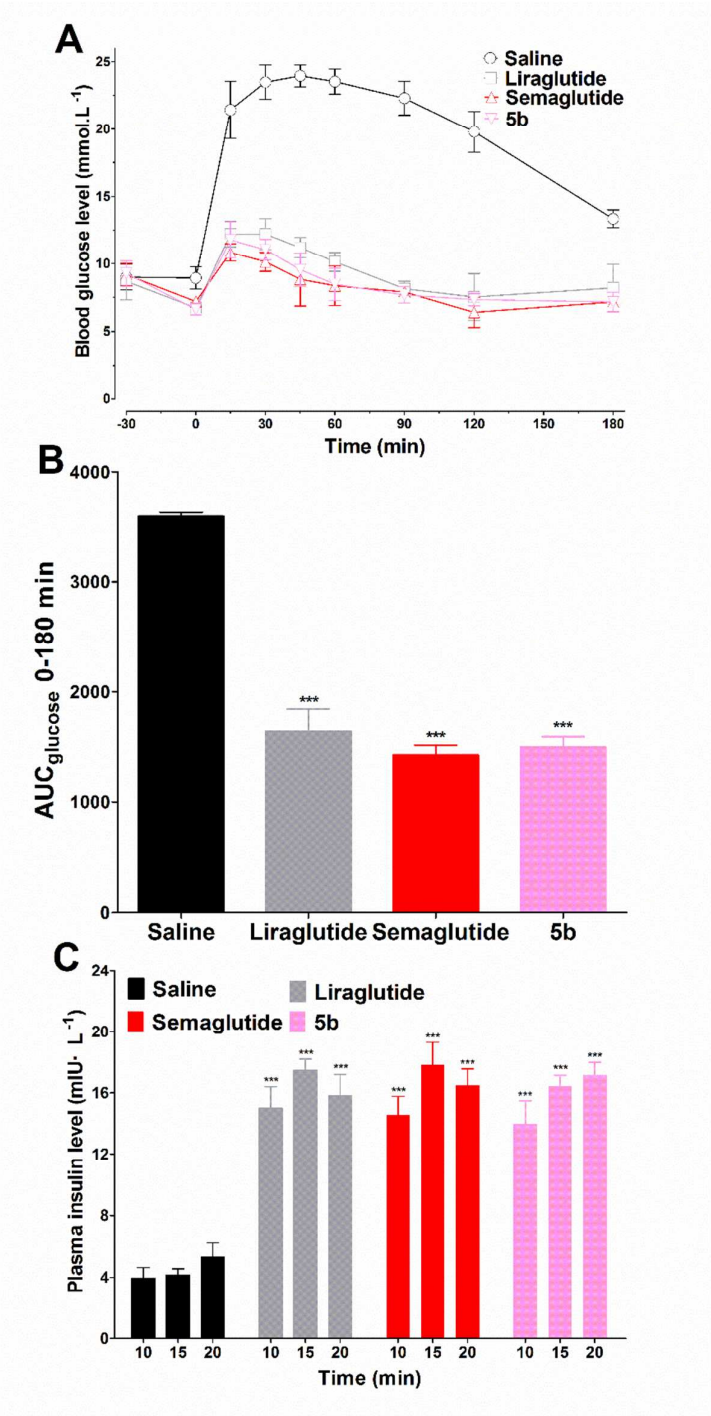

Figure 8. Glucose-lowering and insulinotropic activities of liraglutide, semaglutide and **5b** (25 nmol·kg^{-1}, *i.p.*) tested by IPGTT in *db/db* mice. (A) The course of blood glucose concentrations in each group. (B) $AUC_{glucose\ 0\text{-}180\ min}$ after *i.p.* glucose administration. (C) Plasma insulin levels in each

group of *db/db* mice at 10, 15 and 20 min post *i.p.* glucose load. Means ± SD, n = 6. $^{***}P < 0.001$ *vs.* Saline.

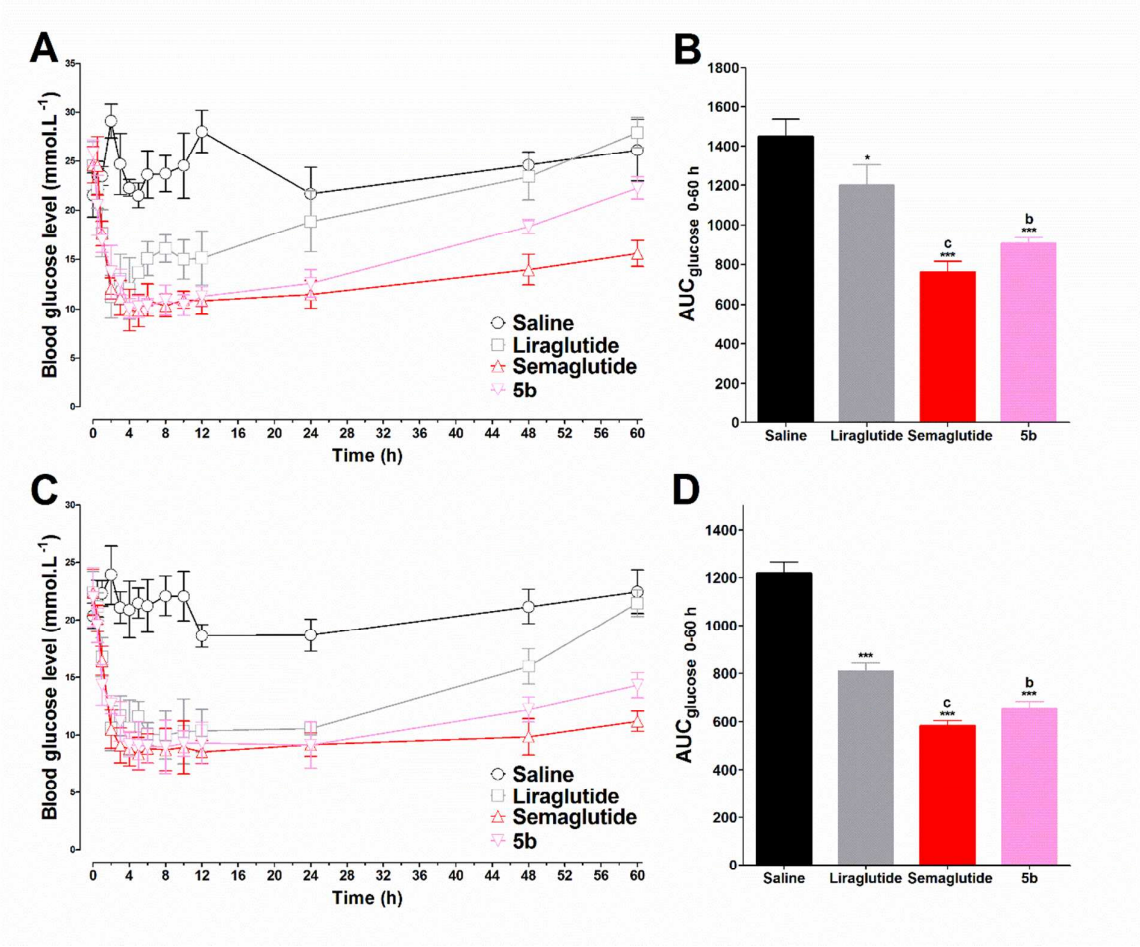

Figure 9. Dose response studies for the hypoglycemic efficacies of liraglutide, semaglutide and **5b** in nonfasted *db/db* mice after *i.p.* dosing of 25 or 150 nmol·kg^{-1}. (A and C) Plots of blood glucose levels of liraglutide, semaglutide and **5b** at the dose of 25 nmol·kg^{-1} (A) or 150 nmol·kg^{-1} (C). (B and D) Calculated glucose $AUC_{0\text{-}60\ h}$ values in each group of mice. Means ± SD, n = 6. $^{*}P < 0.05$ *vs.* Saline, $^{***}P < 0.001$ *vs.* Saline. $^{b}P < 0.01$ *vs.* Liraglutide. $^{c}P < 0.001$ *vs.* Liraglutide.

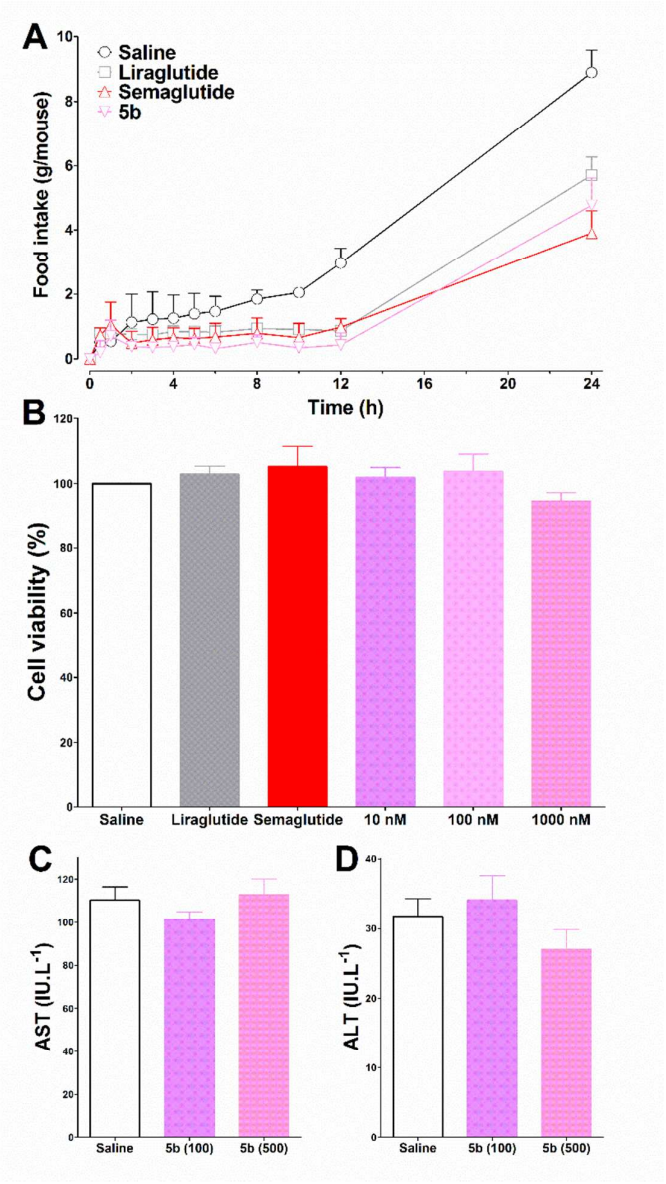

Figure 10. Anorectic and toxicity tests of **5b**. (A) Cumulated food intake (0–24 h) of liraglutide, semaglutide and **5b** (25 nmol·kg^{-1}) in hypoglycemic efficacy tests. Means ± SD, n = 6. (B) Effects of liraglutide, semaglutide (10 nM), and **5b** (10, 100, and 1000 nM) on the viability of INS-1 cells. (C) Acute *in vivo* toxicity of **5b** (100 or 500 mg·kg^{-1}, dosing 2 days) in *db/db* mice. Means ± SD, n = 3.

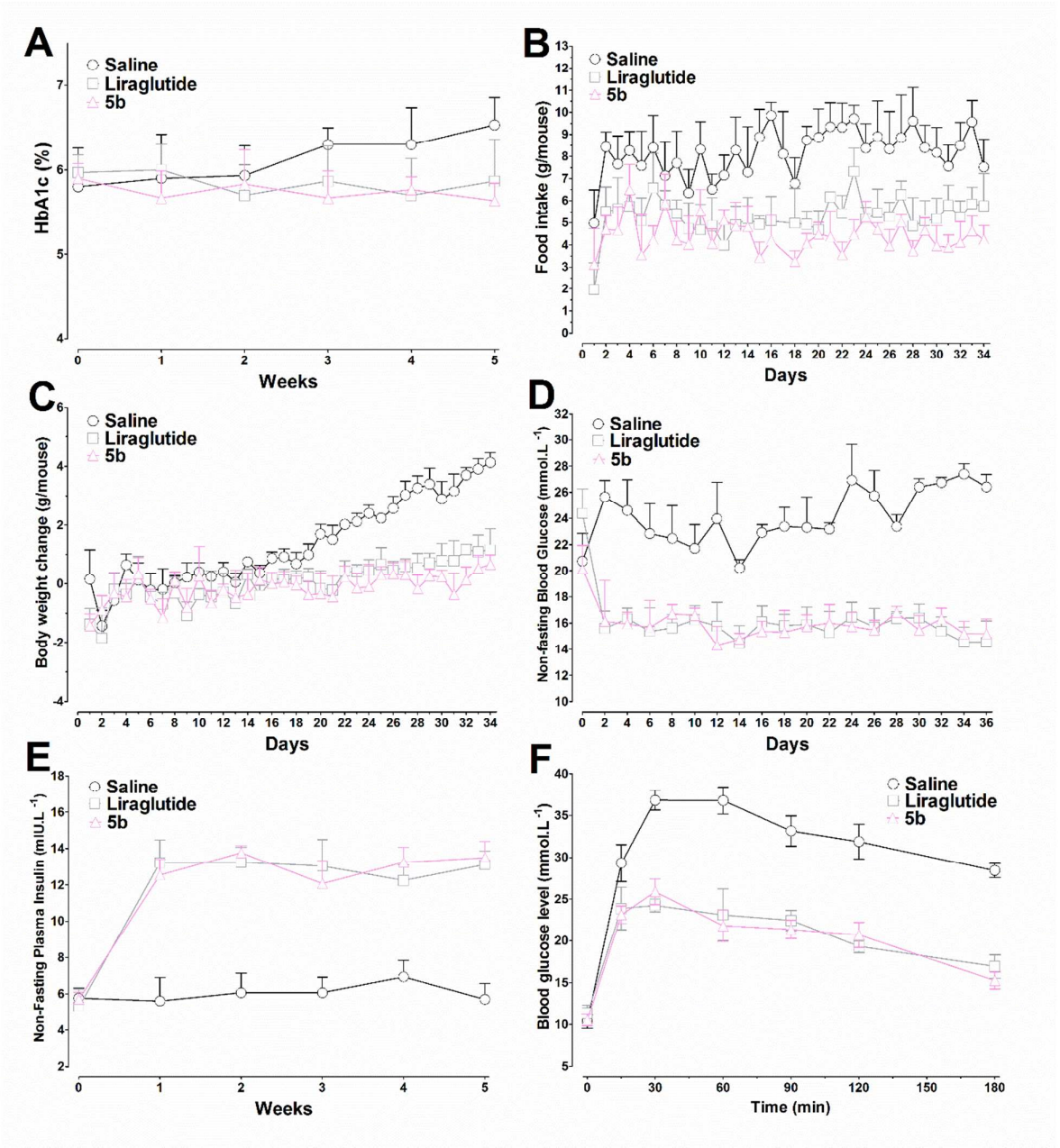

Figure 11. Effects of liraglutide and **5b** on *db/db* mice during a five-week treatment. (A) HbA1c (%) values in each group as measured weekly. (B) Food intake amount (g/mouse). (C) Body weight change (g/mouse). (D) Non-fasting blood glucose concentrations as measured every two days. (E) Non-fasting insulin concentrations as measured every week. (F) IPGTT test performed after the treatment period. Means ± SD, n = 6.

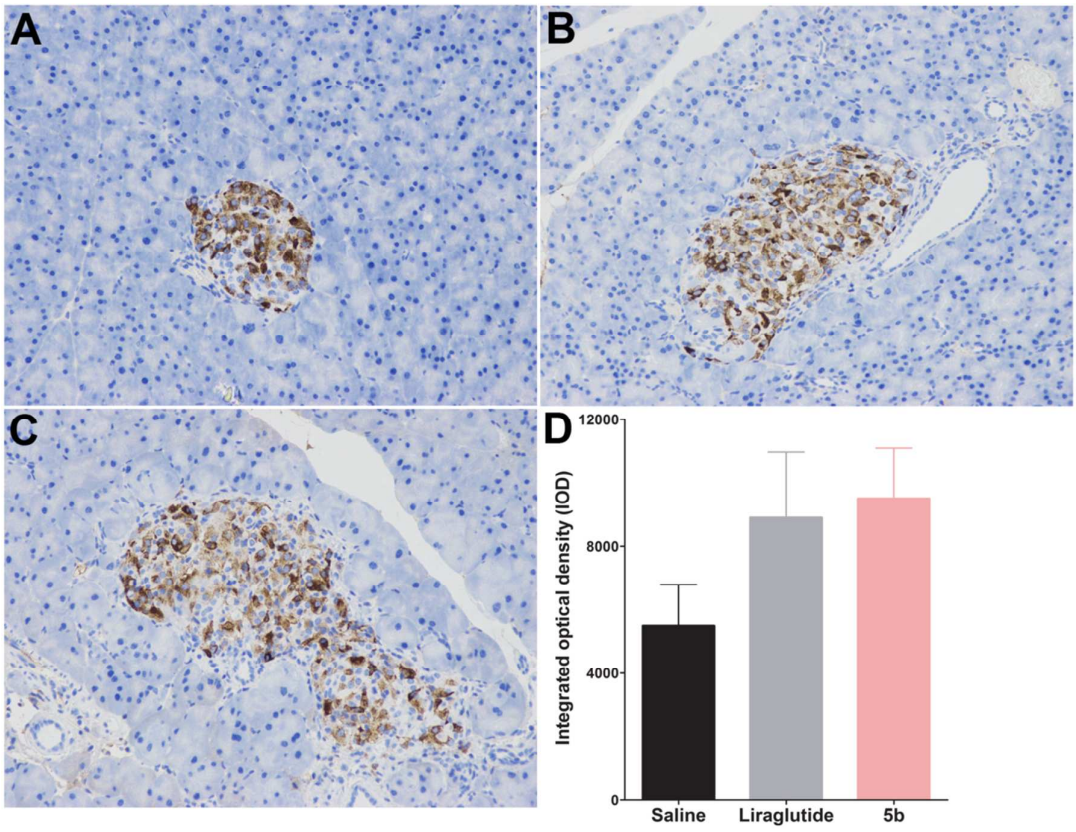

Figure 12. Immunohistochemistry analysis of pancreatic tissue sections in *db/db* mice after five weeks of study. Representative images of insulin immunostaining sections in saline (A), liraglutide (B) and **5b** (C) groups. (D) Integrated optical density (IOD) values of insulin in each group. Data are represented as the Means ± SD for six mice per group.

GLP-1	HAEGT FTSDV SSYLE GQAAK EFIAW LVKGR
Exendin-4	HGEGT FTSDL SKQME EEAVR LFIEW LKNGG PSSGA PPPS
Lixisenatide	HGEGT FTSDL SKQME EEAVR LFIEW LKNGG PSSGA PPSKK KKKK
1	HGEGT YTNDV TEYLE EEAAK EFIEW LIKGK
2	HGEGT YTNDV TEYLE EEAAK EFIEW LIKGK PSSGA PPPS
3	HGEGT YTNDV TEYLE EEAAK EFIEW LIKGK PSSGA PPSKK KKKK
4a	HGEGT YTNDV TEYLE EEAAX_1 EFIEW LIKGK
4b	HGEGT YTNDV TEYLE EEAAX_2 EFIEW LIKGK
4c	HGEGT YTNDV TEYLE EEAAX_3 EFIEW LIKGK
4d	HGEGT YTNDV TEYLE EEAAK EFIEW LIX_1GK
4e	HGEGT YTNDV TEYLE EEAAK EFIEW LIX_2GK
4f	HGEGT YTNDV TEYLE EEAAK EFIEW LIX_3GK
4g	HGEGT YTNDV TEYLE EEAAX_1 EFIEW LIKGK PSSGA PPPS
4h	HGEGT YTNDV TEYLE EEAAX_2 EFIEW LIKGK PSSGA PPPS
4i	HGEGT YTNDV TEYLE EEAAX_3 EFIEW LIKGK PSSGA PPPS
4j	HGEGT YTNDV TEYLE EEAAK EFIEW LIX_1GK PSSGA PPPS
4k	HGEGT YTNDV TEYLE EEAAK EFIEW LIX_2GK PSSGA PPPS
4l	HGEGT YTNDV TEYLE EEAAK EFIEW LIX_3GK PSSGA PPPS
4m	HGEGT YTNDV TEYLE EEAAX_1 EFIEW LIKGK PSSGA PPSKK KKKK
4n	HGEGT YTNDV TEYLE EEAAX_2 EFIEW LIKGK PSSGA PPSKK KKKK
4o	HGEGT YTNDV TEYLE EEAAX_3 EFIEW LIKGK PSSGA PPSKK KKKK
4p	HGEGT YTNDV TEYLE EEAAK EFIEW LIX_1GK PSSGA PPSKK KKKK
4q	HGEGT YTNDV TEYLE EEAAK EFIEW LIX_2GK PSSGA PPSKK KKKK
4r	HGEGT YTNDV TEYLE EEAAK EFIEW LIX_3GK PSSGA PPSKK KKKK

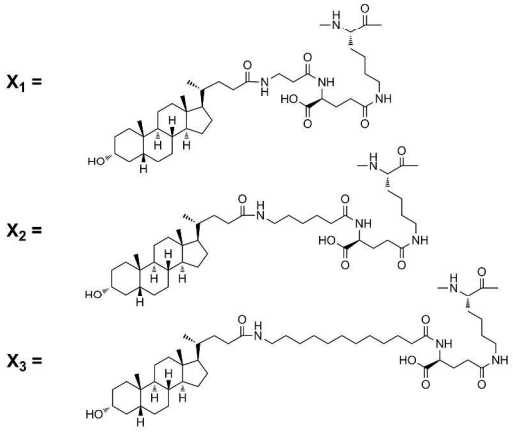

Figure 1. Structures of GLP-1, exendin-4, lixisenatide, peptides 1–3 and conjugates 4a–r.

288x446mm (300 x 300 DPI)

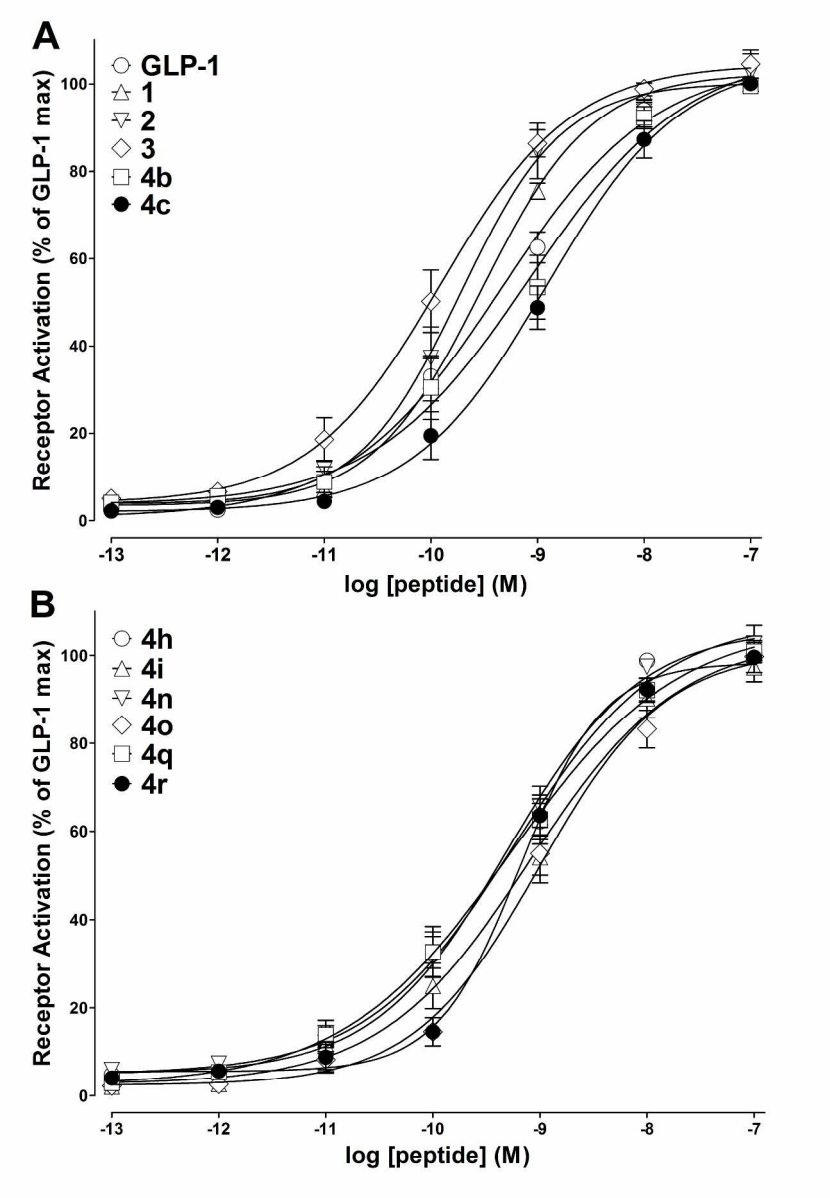

Figure 2. Concentration response curves of GLP-1 and representative LCA-Xenopus GLP-1 conjugates in receptor activation. The data for the test compounds were normalized and plotted as the percentage of maximum cAMP levels stimulated by saturated GLP-1. All experiments were carried out in triplicate and repeated three times (n = 3). Means ± SD.

266x384mm (300 x 300 DPI)

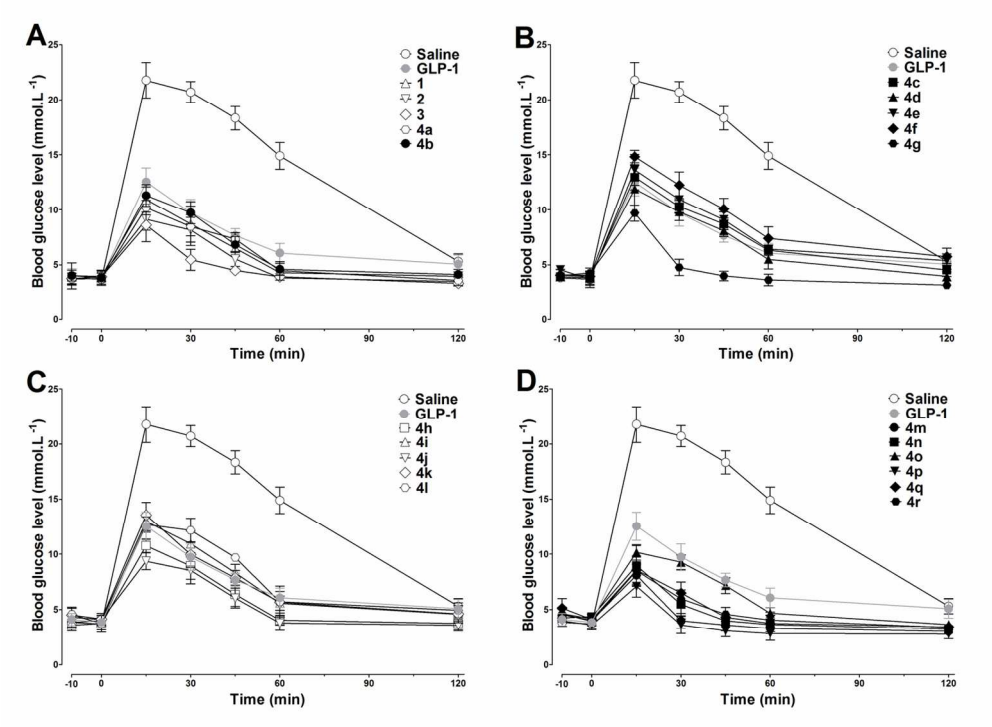

Figure 3. Acute hypoglycemic effects of GLP-1 and 4a–r in Kunming mice. GLP-1 and 4a–r (25 nmol·kg-1) were i.p. loaded at -10 min, followed by i.p. glucose loaded (2 g·kg-1) at 0 min. (A-D) Time-response curves of blood glucose concentrations in each group. Means ± SD, n = 6.

138x101mm (300 x 300 DPI)

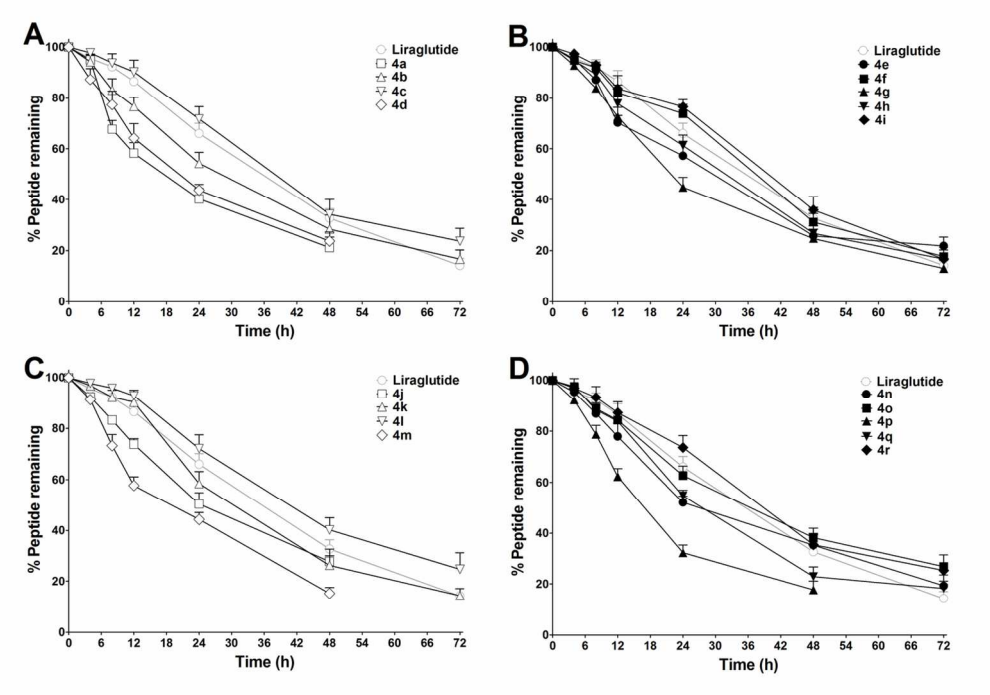

Figure 4. Degradation of liraglutide and 4a–r in rat plasma. Means ± SD, n = 3.

130x91mm (300 x 300 DPI)

5a HGEGT YTNDV TEYLE EEAAX_4 EFIEW LIKGK

5b HGEGT YTNDV TEYLE EEAAX_4 EFIEW LIKGK PSSGA PPPS

5c HGEGT YTNDV TEYLE EEAAK EFIEW LIX_4GK PSSGA PPSKK KKKK

X_4 =

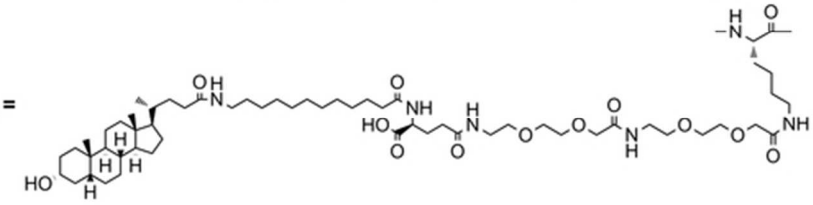

Figure 5. Structures of 5a–c.

51x17mm (300 x 300 DPI)

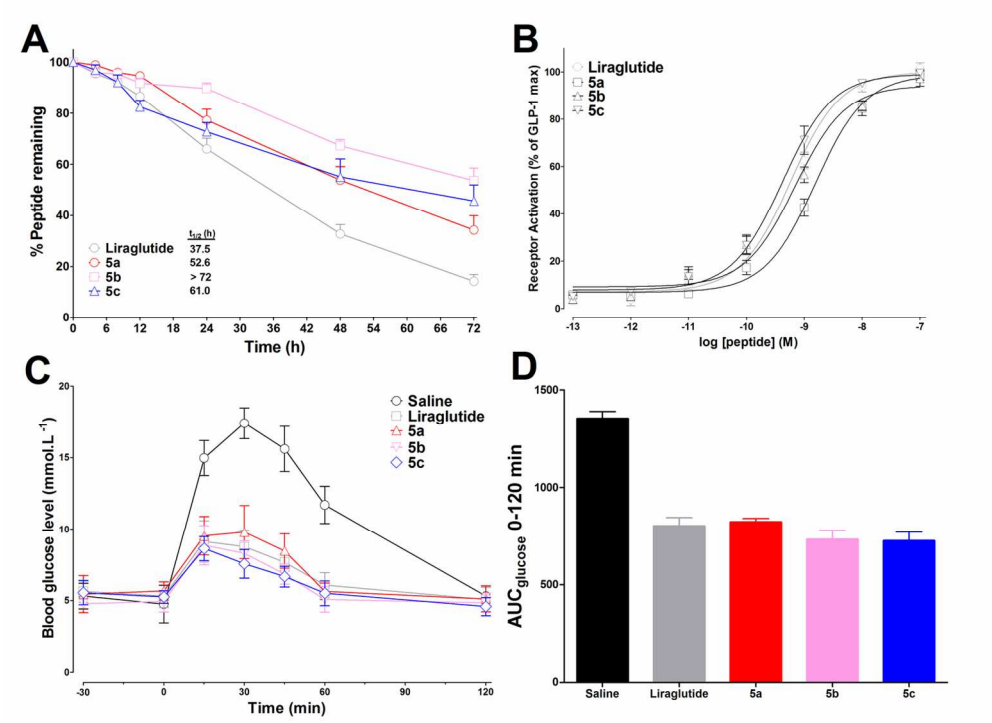

Figure 6. Stability and biological activity tests of 5a–c. (A) Degradation of liraglutide and 5a–c in rat plasma. Means ± SD, n = 3. (B) Concentration response curves of liraglutide and 5a–c in receptor activation. The data for the test compounds were normalized and plotted as the percentage of maximum cAMP levels stimulated by saturated GLP-1. Means ± SD. Experiments were performed in triplicate and repeated three times (n = 3). (C) Time-response curves of blood glucose in liraglutide and 5a–c groups. (D) AUCglucose 0-120 min after i.p. glucose administration. Means ± SD, n = 6.

134x100mm (300 x 300 DPI)

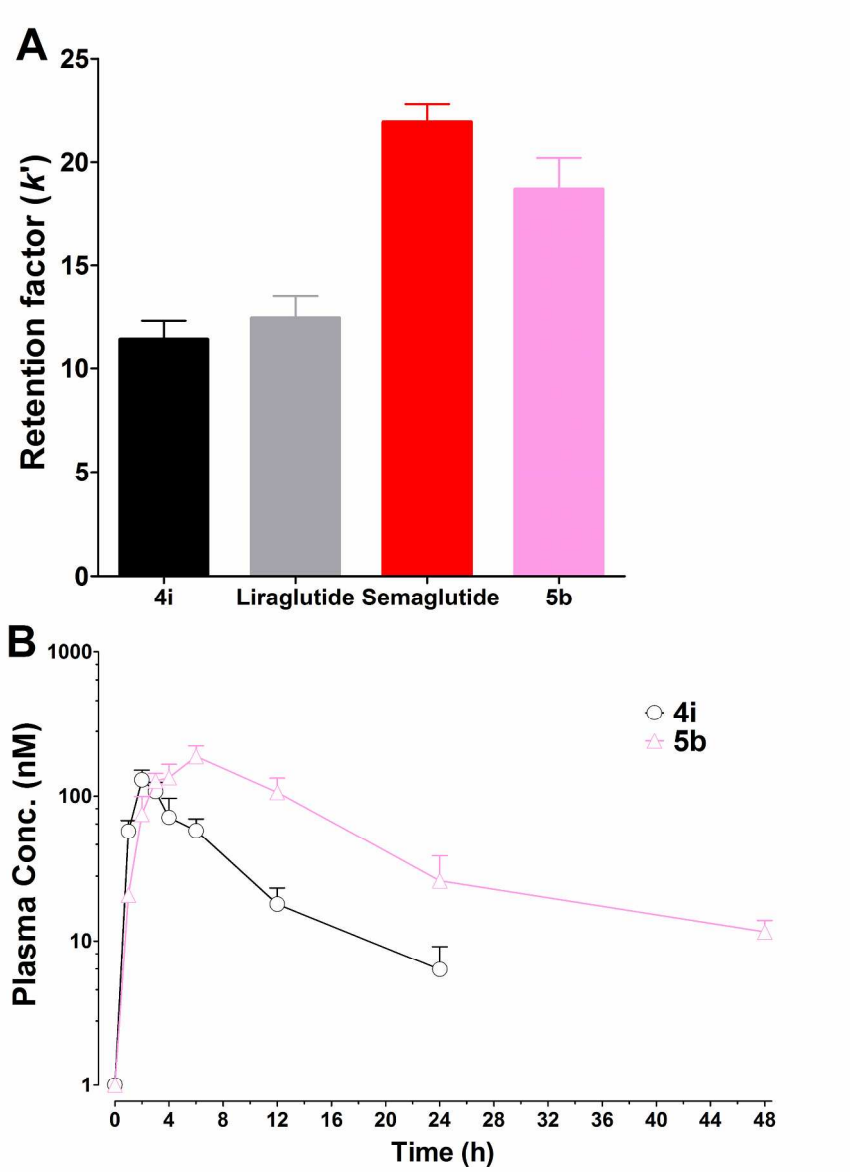

Figure 7. Physicochemical and pharmacokinetic profiles of 5b. (A) The albumin binding affinities of liraglutide, semaglutide, 4i and 5b were measured on HSA HPLC column (k'). (B) Pharmacokinetic profiles of 4i and 5b after s.c. administration in SD rat (50 nmol·kg-1). Means ± SD, n = 3.

230x317mm (300 x 300 DPI)

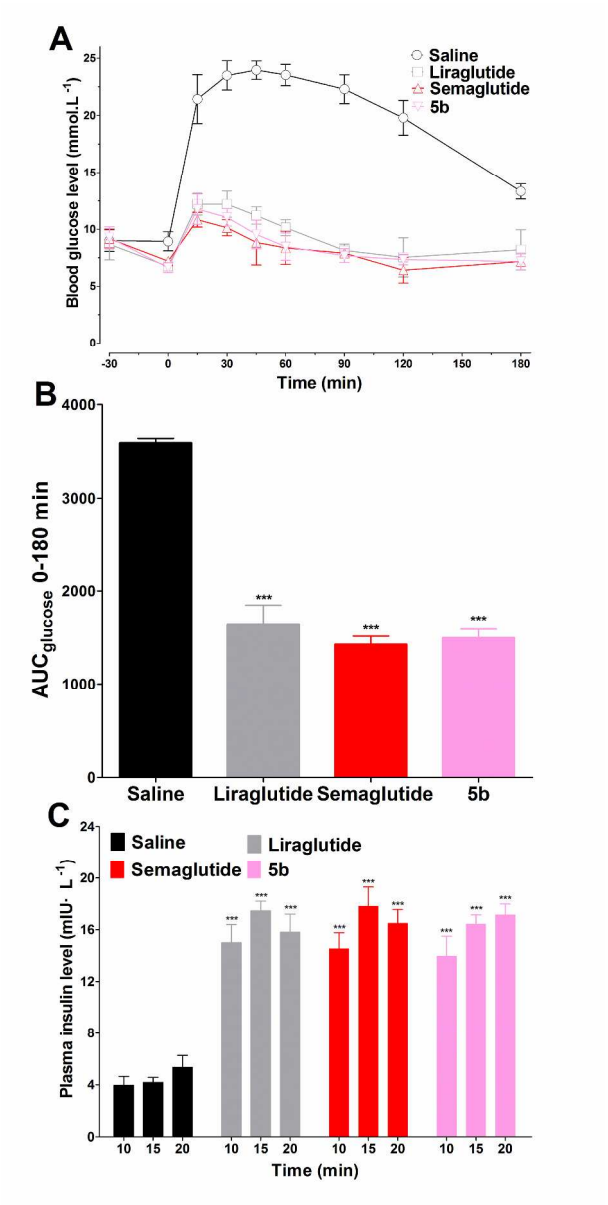

Figure 8. Glucose-lowering and insulinotropic activities of liraglutide, semaglutide and 5b (25 nmol·kg-1, i.p.) tested by IPGTT in db/db mice. (A) The course of blood glucose concentrations in each group. (B) AUCglucose 0-180 min after i.p. glucose administration. (C) Plasma insulin levels in each group of db/db mice at 10, 15 and 20 min post i.p. glucose load. Means ± SD, n = 6. ***P < 0.001 vs. Saline.

279x555mm (300 x 300 DPI)

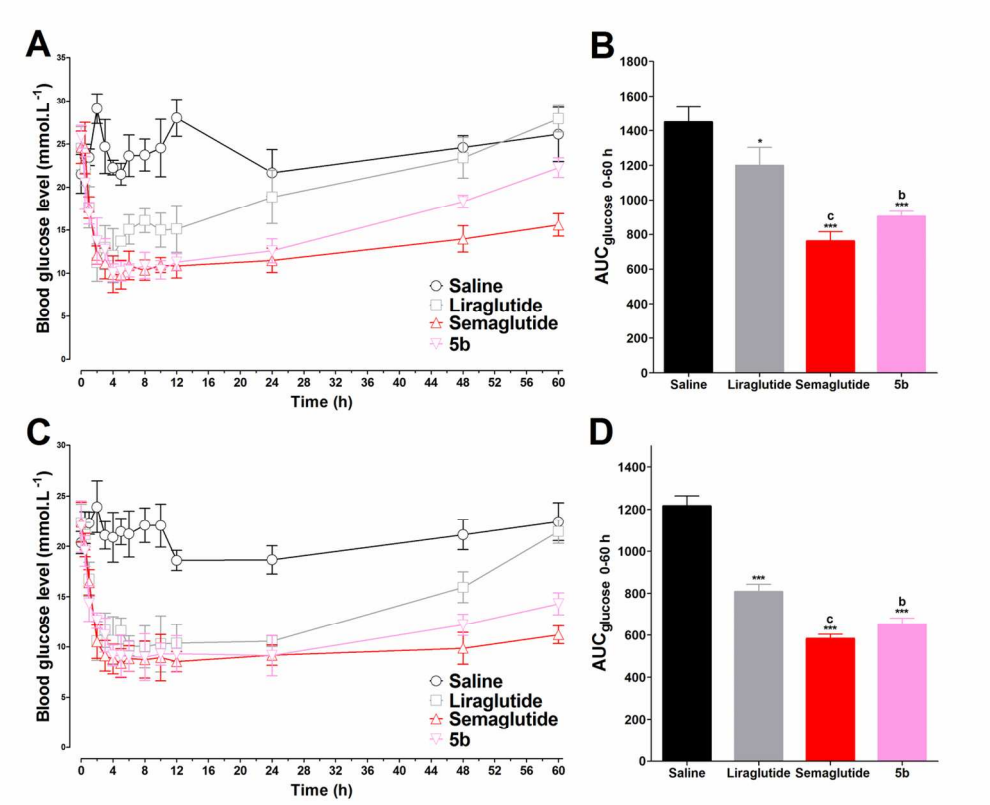

Figure 9. Dose response studies for the hypoglycemic efficacies of liraglutide, semaglutide and 5b in nonfasted db/db mice after i.p. dosing of 25 or 150 nmol·kg-1. (A and C) Plots of blood glucose levels of liraglutide, semaglutide and 5b at the dose of 25 nmol·kg-1 (A) or 150 nmol·kg-1 (C). (B and D) Calculated glucose AUC0-60 h values in each group of mice. Means ± SD, n = 6. *P < 0.05 vs. Saline, ***P < 0.001 vs. Saline. bP < 0.01 vs. Liraglutide. cP < 0.001 vs. Liraglutide.

128x106mm (300 x 300 DPI)

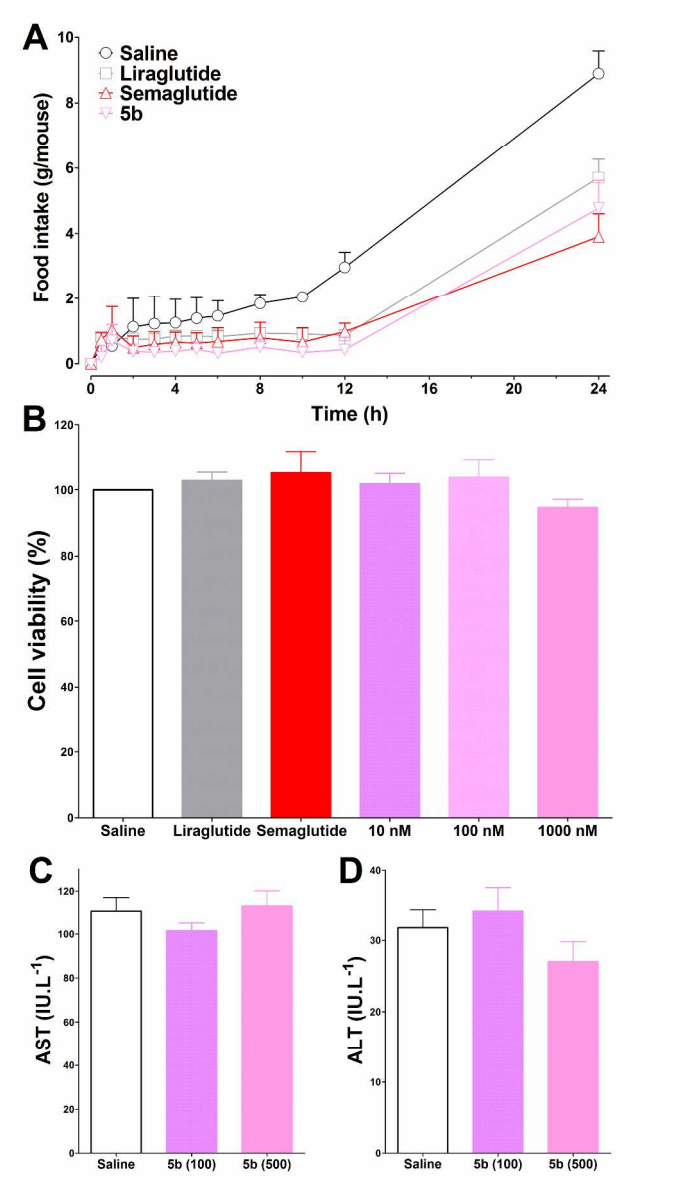

Figure 10. Anorectic and toxicity tests of 5b. (A) Cumulated food intake (0–24 h) of liraglutide, semaglutide and 5b (25 nmol·kg-1) in hypoglycemic efficacy tests. Means ± SD, n = 6. (B) Effects of liraglutide, semaglutide (10 nM), and 5b (10, 100, and 1000 nM) on the viability of INS-1 cells. (C) Acute in vivo toxicity of 5b (100 or 500 mg·kg-1, dosing 2 days) in db/db mice. Means ± SD, n = 3.

260x462mm (300 x 300 DPI)

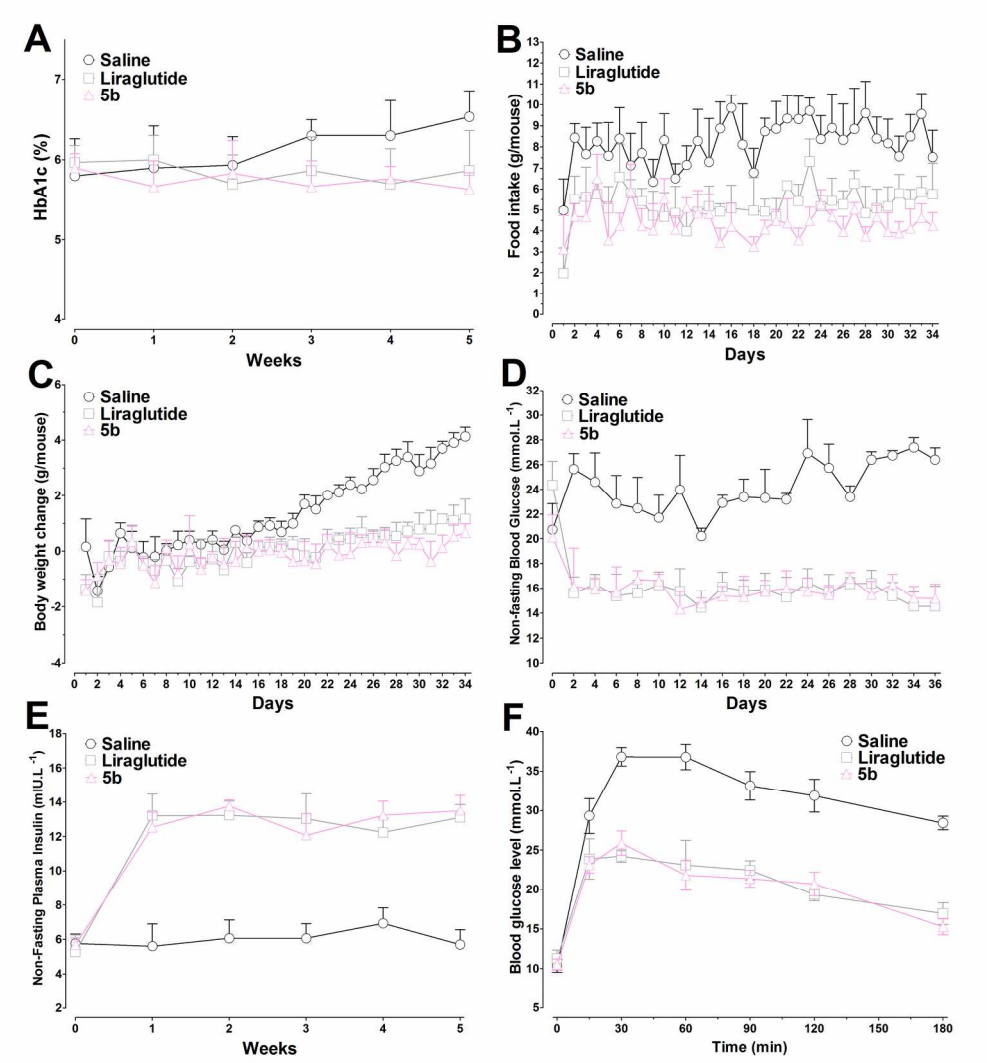

Figure 11. Effects of liraglutide and 5b on db/db mice during a five-week treatment. (A) HbA1c (%) values in each group as measured weekly. (B) Food intake amount (g/mouse). (C) Body weight change (g/mouse). (D) Non-fasting blood glucose concentrations as measured every two days. (E) Non-fasting insulin concentrations as measured every week. (F) IPGTT test performed after the treatment period. Means ± SD, n = 6.

199x216mm (300 x 300 DPI)

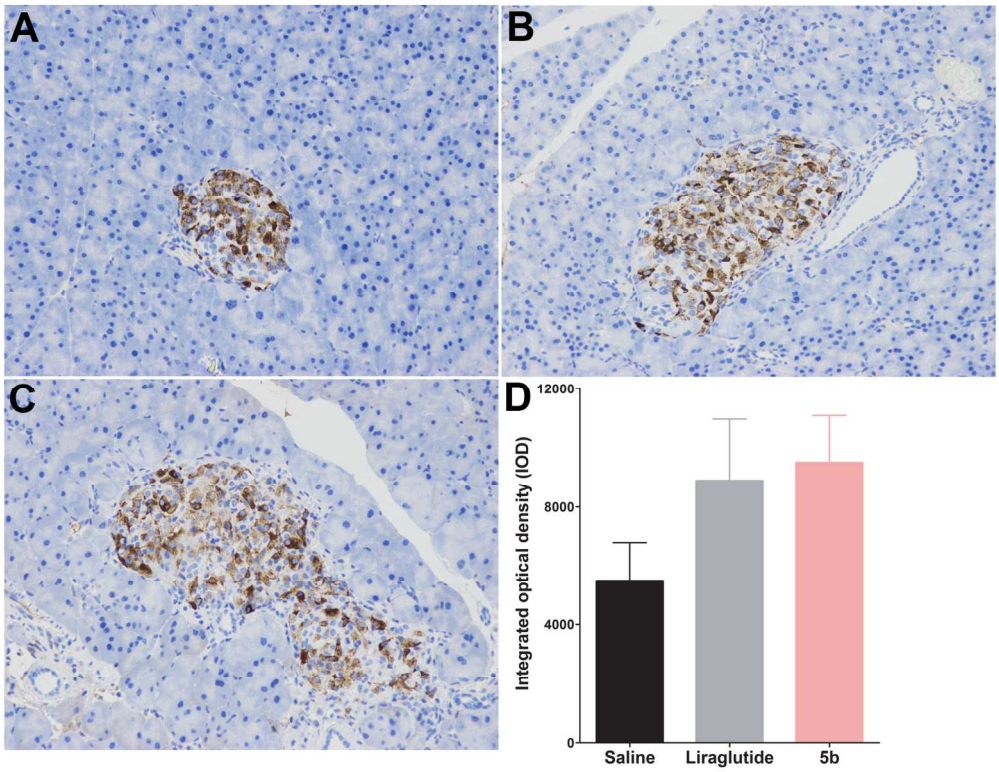

Figure 12. Immunohistochemistry analysis of pancreatic tissue sections in db/db mice after five weeks of study. Representative images of insulin immunostaining sections in saline (A), liraglutide (B) and 5b (C) groups. (D) Integrated optical density (IOD) values of insulin in each group. Data are represented as the Means ± SD for six mice per group.

686x528mm (96 x 96 DPI)

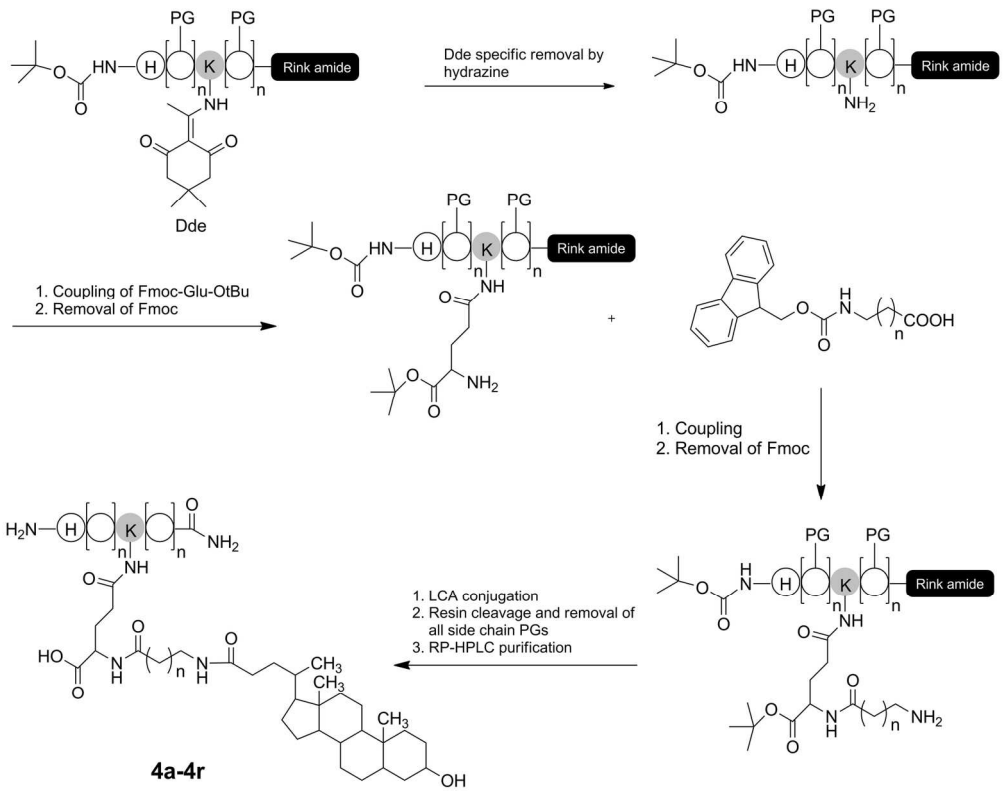

Scheme 1. Synthetic route of 4a–r. PG: Acid labile protecting group.

162x127mm (300 x 300 DPI)

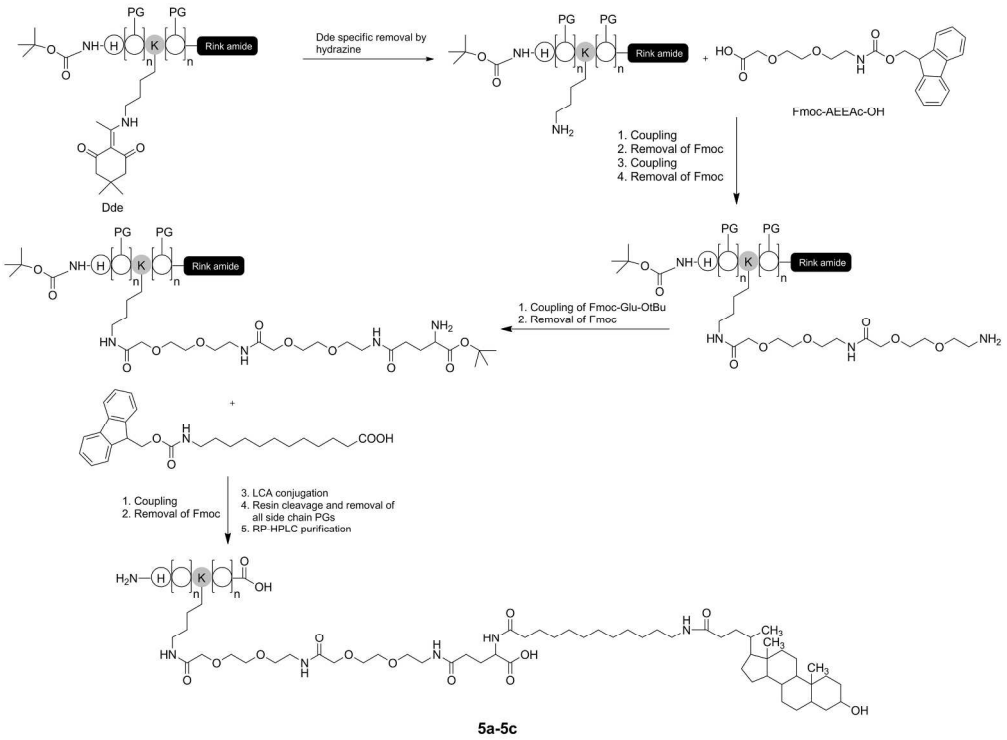

Scheme 2. Synthetic route of 5a–c. PG: Acid labile protecting group.

220x161mm (300 x 300 DPI)